Synthesis and Characterization of Electrodeposited NiO_x Thin Film on Electrode Grade Carbon Plate for Supercapacitor Applications

By

Muhammad Imran Sohail

Reg. No: NUST201362313MSCME67713F

This thesis is submitted as a partial fulfillment of the requirements for the degree of

MS in Materials and Surface Engineering

Supervisor Name: Dr. Zakir Hussain

School of Chemical and Materials Engineering (SCME)

National University of Sciences and Technology (NUST), H-12

Islamabad, Pakistan

July 2017

Dedication

I would like to dedicate this thesis to my loving wife and kids who suffered a lot during my research work but always supported me in difficult times and never let me down.

I am also grateful to my mother for her constant prayers and encouragement which always motivated and strengthened me to complete this task.

Acknowledgement

First, my acknowledgement goes to Almighty **ALLAH** WHO granted me the wisdom and passion to execute my research work.

Secondly, I would like to acknowledge my supervisor **Dr. Zakir Hussain** who motivated and supported me for this research topic. He provided me all the resources, both financially and technically, to carry out this research. He always guided and encouraged me to overcome all the barriers that came in my way to accomplish this job.

I would also like to acknowledge my committee members, **Dr. Muhammad Shahid** who granted me permission to work in Corrosion Lab. and **Dr. Muhamad Mujahid** for appreciating my research idea and his valuable motivation.
Moreover. I want to acknowledge **Dr. Iftikhar Hussain Gul,** who not only solved my administrative issues as a PG Coordinator but also supported me during Lab work and characterization of samples, and **Dr. Aftab** for giving valued suggestions to evaluate my results of cyclic voltammetry.

The last but not the least, I acknowledge all the faculty members, nonteaching staff and especially, **Mr. Abdul Qadeer** who imparted me his skills as a Lab Engineer to perform my experimental work and **Mr. Zarar Khan** for his support during late sitting hours in Labs and his assistance at various phases throughout this struggle.

M. Imran Sohail

Abstract

The uniform NiO thin film composed of interconnected submicron sized granular particles with dense morphology is successfully electrodeposited on electrode grade carbon plate through electrochemical strategy. In the first stage, Nickel oxide/hydroxides are synthesized on the carbon substrate in 0.15M Nickel Nitrate hexahydrate[$Ni(NO_3)_2 .6H_2O$] aqueous electrolyte. In the second stage, as synthesized film is annealed at 250^0C @ 5^0C/min in a muffle stove to completely convert any existing hydroxides to nickel oxide. The microstructures, phase and surface composition are investigated through SEM, XRD and EDX. Electrochemical performance of NiO modified carbon electrode was evaluated through CV. The specific capacitance of carbon electrode was estimated to be enhanced from 4 F/g to 254 F/g in 1M KOH electrolyte with electrochemical deposition of thin porous NiO film. The linear behavior of maximum anodic current with scan rate shown by CV curves confirmed the ideal electrode performance for supercapacitor applications.

Contents

List of Figures

List of Tables

Chapter 1

Introduction

1.1 Motivation

Due to its seasonal advantage, Pakistan has the potential for solar energy and wind energy, known as clean energy resources, in bulk but to utilize these energy resources efficiently development of energy conversion and storage devices indigenously is a big challenge for us to overcome our national energy crisis. Regarding conversion of chemical and solar energy into electricity, there is a need to focus and enhance the research activities on progress in technology of various types of solar cells including silicon based solar cells; polymer and Perovskite based solar cells as well as fuel cells. In addition to this, to conserve the energy formed by these devices, maturity of energy storage is equally important. Currently nano-technology is being employed to increase the capacity of energy storage materials. For example, supercapacitor electrodes are manufactured through synthesis of nano- structured thin films on suitable substrates.

The focus of the current research is continuously increasing on synthesis of single/binary transition metal oxide thin films based on low cost earth abundant metals like Ni, Co, Mn, Fe, and Cu etc. by electrodeposition technique and tailor their properties through control of morphology and chemical composition. The introduction of these low-cost materials in place of expensive ones like Ru, Pt, lr etc. in energy storage devices e.g. batteries and fuel cells will be cost effective and helpful for commercialization of these devices. Electrodeposition is an economical, precise and versatile technique for synthesis of nano-particulate thin films with different morphologies and compositions. The nanostructured materials show enhanced electrochemical reaction activity at electrode-electrolyte interface required during redox process for increased energy density and power density in energy storage devices. Electrodeposition was performed in aqueous solutions which is strongly dependent on pH value of the solutions [1, 2]. Additionally, the electrodeposition of transition metal oxides in aqueous electrolytes is also influenced by key factors such

as temperature [3], current density [4] and chemical composition of electrolyte [3] as well as type of substrate.

1.2 Energy storage devices

The deposition of thin film on a substrate at nano scale through electrochemical technique permits the use of low amount of metal charge as well as control over size and morphology of nanoparticles. The electrochemical technique has been successfully employed to produce nano-structured thin films on a variety of substrates for supercapacitor electrodes. Supercapacitors are part of advanced energy storage systems which are under focus of current research activities [5]. Super capacitors, also known as ultracapacitors or redox electrochemical capacitors, provide efficient storage of electrical energy for clean and renewable energy sources like solar energy, wind farms as well as fuel cells. Currently, Hybrid gasoline-electric vehicles (HEV) [6-8] have become the highly demanding field for supercapacitor applications.

Various inorganic and organic materials like conducting polymers have been employed as electrode materials for Supercapacitors. In the case of inorganic materials, various noble and transition metal oxides have been tried as electrodes in electrochemical capacitors out of which RuO2 proved to be the winner exhibiting a specific capacitance of ~720 F/g [9]. However, the high cost as well as scarcity of ruthenium oxide is a barrier for its commercialization as an electrode material for Supercapacitors.

Amongst transition metal oxides, Nickel oxide is a premium candidate for electrode material basically due to its high electrochemical performance along with its economy and natural abundance [10]. The interest in NiO cropped up due to its high theoretical value of super-capacitance (~3228 F/g). A multiple of synthesis techniques have been employed in the past to achieve diverse kind of NiO structures, including chemical precipitation method, electrophoresis, electrochemical deposition, sol-gel process, hydrothermal route and co-precipitation schemes. The structures produced were loose-packed flake like, nano-flakes as well as nanofibers having versatile pore sizes like open macropores, mesopores and nanopores. The maximum specific capacitance achieved by exploiting the above techniques reaches ~942F/g [11].

Presently the research is focused on producing nano-structured materials for electrodes because extremely high surface to volume ratio at nano-scale enhances the active material which contributes in electrochemical electrode-electrolyte interaction [12]. In addition to this, the diffusion path for transport of electrolyte ions into the active material for electrochemical reaction becomes shorter thus increasing the reaction rate [13]. Therefore, it is vital to manipulate the microstructures of NiO through various tactics to enhance the specific capacitance of NiO near to its theoretical value [14]. The high performance NiO electrodes will increase the energy density and power density of supercapacitors.

1.3 Role of Electrochemistry

The study of charge transfer between a molecule/atom dissolved in a conductive electrolyte and electrode is the essence of electrochemistry. The scientists working on electrochemistry have established the conditions and standards under which electron transfer reactions take place and can be reproduced. By using the established electrochemical data, various combinations of electrode materials and electrolytes can be engineered to electrodeposit a variety of materials as well as their compounds. These species are deposited on the electrode by electron transfer reactions, commonly known as redox reactions, taking place between the ions (charged atoms/molecules) that are dissolved in electrolyte and electrodes.

The energy is needed to charge a neutral atom or molecule to convert it into its ionic state. This threshold energy which is known as Born salvation energy [15] can be calculated by using the following equation;

$$\mu_i = - z^2e^2/8\pi\varepsilon_0 a\,[1- 1/\varepsilon\,] \qquad (1.1)$$

Where, ze= charge carried by the ion

a=radius of ion in a medium of dielectric constant, ε.

The energy μi is the energy required to produce an ion from neutral atom into water. This energy is basically the difference between energy acquired to discharge an ion in vacuum and the energy needed to charge the ion in solvent. Actually, spontaneous ionic organization takes place in a salt to minimize the electrostatic energy. To understand the formation mechanism of ionic solution from a source salt, insight study of free energy and entropy changes accompanied with this phenomenon is essentially

required. For instance, high entropy value of ions in a solution causes the quick dissolution of salt into the solvent.

1.4 Electrode Potentials

If any metal is dipped in water, its ions are soluble in water but not metal it. The formation of these ions is due to an inherent driving force caused by entropy. However, when an ion goes into water, two electrons are produced for example in case of Magnesium electrode. These electrons remain on the electrode surface and increase the potential of the electrode. This development progresses until the point when electrode acquires a threshold potential where no further electrons are bestowed to the metal. This stage is attained when Fermi level of the metal electrode is precisely in equilibrium with potential of the electrolyte [16]. In other words, as concentration of the ions in the solution increases, their free energy increases which can be related to the logarithm of this concentration. Finally, both reaction rates taking place become equal.

These reactions can be illustrated as below;

Reaction I: Metal $\longrightarrow$ Ion+ Electrons

Reaction II: Ion + Electrons $\longrightarrow$ Metal

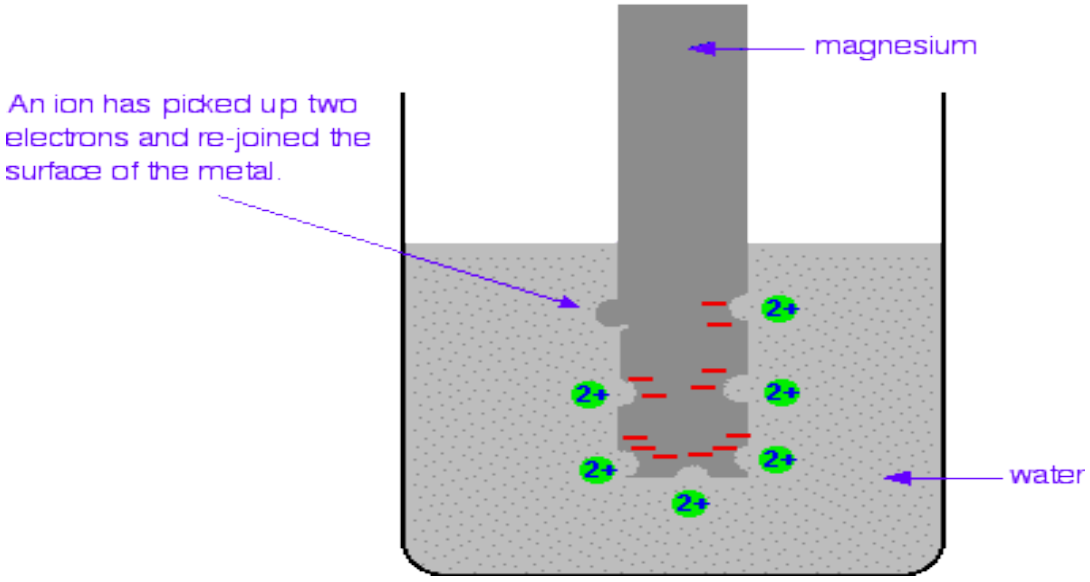

Figure 1.1 Equilibrium b/w metallic atoms of an electrode and ions soluble in an aqueous solution. [16]

The final potential up to which an electrode reaches when it is immersed into a solution of known concentration of ions in equilibrium with the electrode has a standard value. The threshold energy required to take away an electron from the metal is equivalent to the average of the work performed in producing a positively charged ion and work achieved in neutralizing it to get equilibrium between Fermi level of the electrode material and potential of electrolyte. Due to production of electrons the charge builds up on the electrode surface which causes the shifting in Fermi level of metal as per Poisson's Equation. This surface charge is balanced by collection of ions close to electrode surface. This mechanism results in a double layer at the electrode-electrolyte interface. The double layer can be illustrated by the Debye model in Figure 1.2.

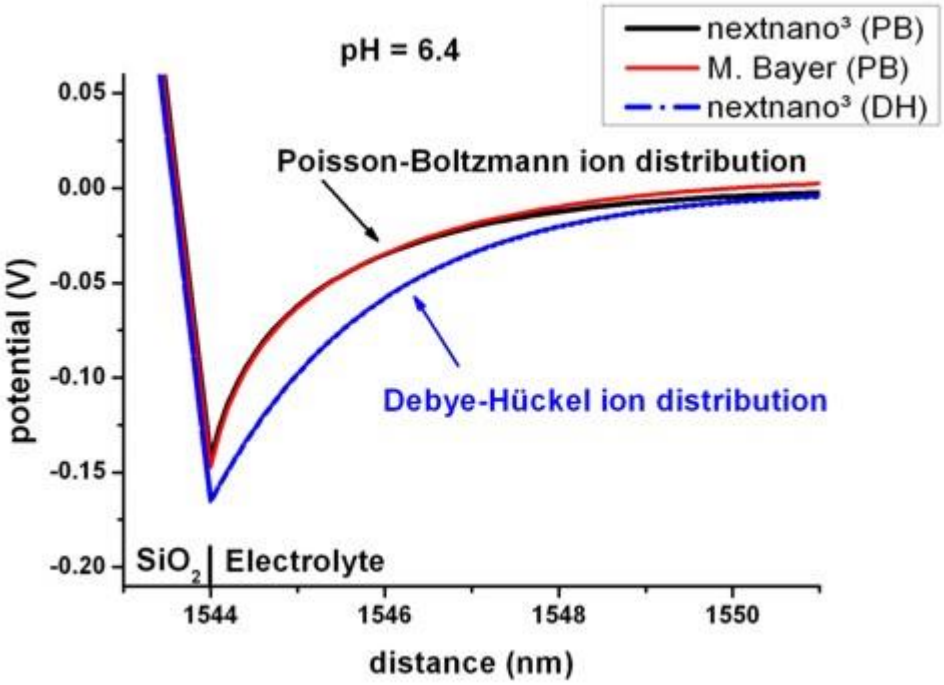

Figure 1.2 Distribution of ions in electrolyte [15]

The standard electrode potentials have been measured relative to vacuum. These potentials are calculated with the help of a reference electrode which comprises of a "standard metal" in touch with a "standard" solution of ions through some "standard" boundary. SHE (Standard hydrogen electrode) is an example of a reference electrode in which platinum metal is in contact with a standard aqueous solution of H_2 gas. This solution is made by simmering hydrogen gas into the solution at ambient pressure.

Platinum has the capability to absorb hydrogen and thus makes a pool of H_2 molecules which are in equilibrium with hydrogen ions in the water. If a very small amount of current is passed through this platinum electrode, a potential difference results between the electrode and the solution having a standard value depending on the fixed concentration of hydrogen molecules and protons present at the surface of the electrode. This scheme of reference electrode is illustrated in Figure 1.3.

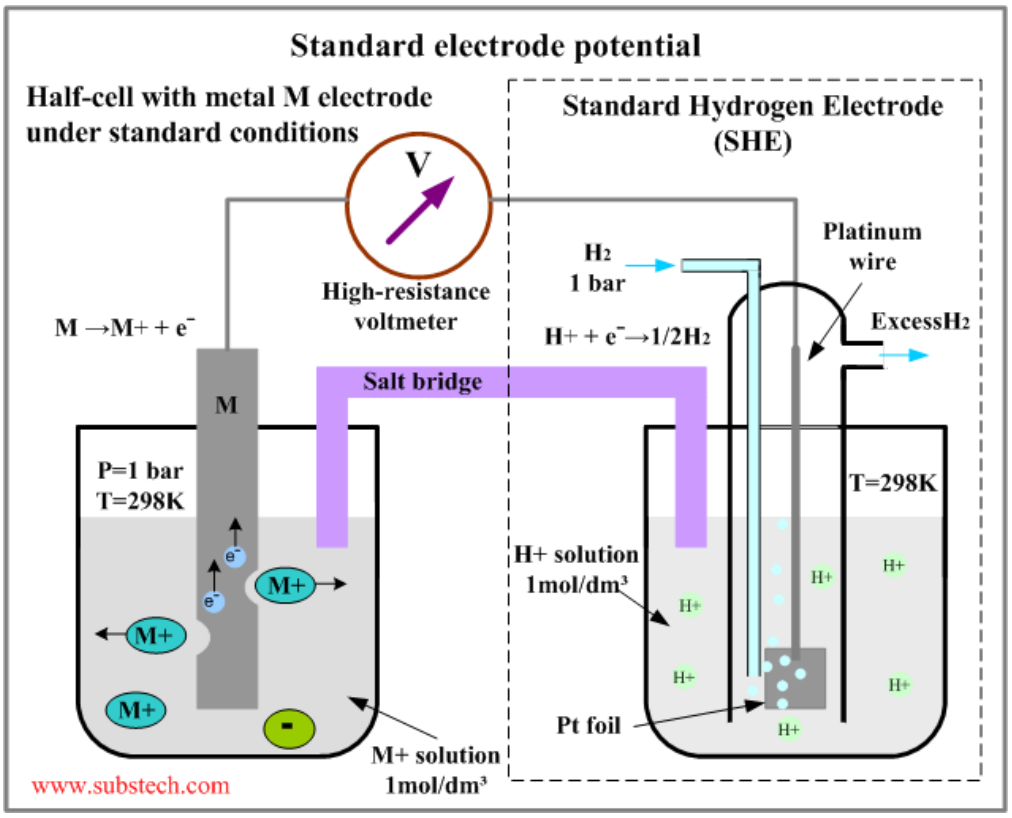

Figure 1.3 Plan for measuring the standard potential of a metal electrode in equilibrium with standard salt solution vs a reference electrode. The salt bridge functions in such a way that it stops the pollution of the two solutions until they reach at equilibrium with each other. [15]

The left section of the diagram shows the construction of reference electrode. The hydrogen gas is bubbled in which is absorbed by porous platinum immersed in 1M acid which provides 1M H^+ at the electrode surface under ambient pressure. In the right compartment a monovalent metal electrode is dipped in its own salt solution which is in equilibrium with the metal. The production of cations produces electrons

which increase the potential of metal electrode. The potential difference between the electrodes supplies the driving force for the redox reaction;

$$2M\ (solid)\ -2e^{-} \longrightarrow 2M^{+}$$

The reaction on the opposite electrode occurs as follows;

$$2H+\ (aq)\ +2e^{-} \longrightarrow H_2\ (gas)$$

A high impedance voltmeter when connected between the electrodes measures this potential. The requirement for high impedance results from the fact that this type of voltmeter draws almost negligible current to maintain the equilibrium of ions undisturbed in the two half cells. At the stage when there is equilibrium between the two electrodes no ion movement occurs. This system behaves as a battery when the voltmeter is exchanged by a load because it draws current thus perturbing the equilibrium potential until the reactants in the half cells are consumed. This plan solves the problem of measuring potentials relative to vacuum. Additionally, the potentials measured relative to the SHE can also be linked to the potentials calculated relative to the vacuum. One method adopted to perform such kind of measurement was shifting of electrode from electrochemical cell to a vacuum chamber having ultrahigh vacuum where ultraviolet photoemission extent was assessed to resolve the work function of the electrode. The result was that the Fermi level of SHE rests ~4.4V below that of vacuum. In addition to SHE, various other types of reference electrodes also exist. For example, Ag/AgCI (SSCE) which consist of silver wire in touch with solid AgCI which in turn have a standard AgCI solution in equilibrium. If the quantity of solid silver chloride in contact with silver wire does not change and the concentration of the standard silver chloride solution is kept invariable, then the potential difference between the silver metal and salt solution remains unchanged. This type of interface has stable polarization and in electrochemistry the electrodes having this kind of interface are known as ideal non- polarizable electrodes.

Therefore, in electrochemistry the potential of the working electrode is measured relative to the fixed potential of the reference electrode by connecting a voltmeter of very high impedance between the two respective electrodes. By using this scheme the standard electrode potentials are measured for all metals. The prime advantage of this standard scale comes in two ways, one is the quantification of energy required for

transfer of electrons and the other is identification of electrodes who will donate the electrons and who will accept the electrons during electrochemical reaction. As depicted in Figure 1.1, the equilibrium was established between Mg metal and its ions present in electrolyte. It is also interesting to note that ions of a metal having different oxidation states can also have equilibrium with each other, for example Fe2+ and Fe3+. It is not necessary for an electrode to take part in the reaction directly. The example is noble metal electrodes of Au and Pt which are for instance in contact with an aqueous solution of Fe^{2+} and Fe^{3+} ions. In this case the potential is independent of the electrode material because it does not react with the ions of the solution. The reason of this phenomenon is due to the formation of a polarization layer on the noble metal surface which equates the Fermi level of the metal with the potential of the electrolyte. Thus, the standard potentials measured with the help of these reference electrodes provide exact values to convert a metal atom into its ion as well as to exchange different oxidation numbers of an ion. The standard reduction potentials of some selected metals measured with respect to standard hydrogen electrode (SHE) in aqueous medium are listed in Table 1.1.

Entire reactions shown in Table 1.1 are half-cell reactions of the whole electrochemical cell that consist of working electrode as well as reference electrode. The logic behind this is the fact that one electrode loses electrons in one half cell reaction and the second electrode receives these electrons to preserve charge neutrality in the other half cell reaction. These electron acceptor reactions are shown in Table 1.2 with standard potentials of reduction. SHE (Standard hydrogen electrode) is the second electrode in these reactions used as a reference electrode.

Standard potentials are identified for accurately equal quantities of reactants and products taking part in redox reaction for a specific electrode. For non-equilibrium ratio of concentrations, the drift in standard potential can be measured based on free energy change which is dependent on concentration of species.

$$\Delta G=\Delta G^0 + RT \ln Q \qquad (1.2)$$

Where ΔG^0 is standard molar free energy, equal to the difference between the free energy of one mole of reactants and products given by the equation, $\Delta G^0=G^0R - G^0P$ where subscripts R & P denote the reactants and products. "R" is the universal gas

constant. The negative value of standard molar free energy implies that the products possess a lesser free energy than reactants. "Q" is termed as reaction quotient.

Table 1.1 List of standard potentials required for electron transport reactions during reduction process. The symbol " ⟶ " shown in the reaction signifies that reactants and products are in equilibrium with each other at a standard electrode potential (E^0) regarding the SHE (The reduction of H^+ at 0V). [16]

Standard Reduction Potentials at 25°C (298 K) for Many Common Half-reactions

Half-reaction	$\mathscr{E}°$ (V)	Half-reaction	$\mathscr{E}°$ (V)
$F_2 + 2e^- \rightarrow 2F^-$	2.87	$O_2 + 2H_2O + 4e^- \rightarrow 4OH^-$	0.40
$Ag^{2+} + e^- \rightarrow Ag^+$	1.99	$Cu^{2+} + 2e^- \rightarrow Cu$	0.34
$Co^{3+} + e^- \rightarrow Co^{2+}$	1.82	$Hg_2Cl_2 + 2e^- \rightarrow 2Hg + 2Cl^-$	0.27
$H_2O_2 + 2H^+ + 2e^- \rightarrow 2H_2O$	1.78	$AgCl + e^- \rightarrow Ag + Cl^-$	0.22
$Ce^{4+} + e^- \rightarrow Ce^{3+}$	1.70	$SO_4^{2-} + 4H^+ + 2e^- \rightarrow H_2SO_3 + H_2O$	0.20
$PbO_2 + 4H^+ + SO_4^{2-} + 2e^- \rightarrow PbSO_4 + 2H_2O$	1.69	$Cu^{2+} + e^- \rightarrow Cu^+$	0.16
$MnO_4^- + 4H^+ + 3e^- \rightarrow MnO_2 + 2H_2O$	1.68	$2H^+ + 2e^- \rightarrow H_2$	0.00
$IO_4^- + 2H^+ + 2e^- \rightarrow IO_3^- + H_2O$	1.60	$Fe^{3+} + 3e^- \rightarrow Fe$	−0.036
$MnO_4^- + 8H^+ + 5e^- \rightarrow Mn^{2+} + 4H_2O$	1.51	$Pb^{2+} + 2e^- \rightarrow Pb$	−0.13
$Au^{3+} + 3e^- \rightarrow Au$	1.50	$Sn^{2+} + 2e^- \rightarrow Sn$	−0.14
$PbO_2 + 4H^+ + 2e^- \rightarrow Pb^{2+} + 2H_2O$	1.46	$Ni^{2+} + 2e^- \rightarrow Ni$	−0.23
$Cl_2 + 2e^- \rightarrow 2Cl^-$	1.36	$PbSO_4 + 2e^- \rightarrow Pb + SO_4^{2-}$	−0.35
$Cr_2O_7^{2-} + 14H^+ + 6e^- \rightarrow 2Cr^{3+} + 7H_2O$	1.33	$Cd^{2+} + 2e^- \rightarrow Cd$	−0.40
$O_2 + 4H^+ + 4e^- \rightarrow 2H_2O$	1.23	$Fe^{2+} + 2e^- \rightarrow Fe$	−0.44
$MnO_2 + 4H^+ + 2e^- \rightarrow Mn^{2+} + 2H_2O$	1.21	$Cr^{3+} + e^- \rightarrow Cr^{2+}$	−0.50
$IO_3^- + 6H^+ + 5e^- \rightarrow \frac{1}{2}I_2 + 3H_2O$	1.20	$Cr^{3+} + 3e^- \rightarrow Cr$	−0.73
$Br_2 + 2e^- \rightarrow 2Br^-$	1.09	$Zn^{2+} + 2e^- \rightarrow Zn$	−0.76
$VO_2^+ + 2H^+ + e^- \rightarrow VO^{2+} + H_2O$	1.00	$2H_2O + 2e^- \rightarrow H_2 + 2OH^-$	−0.83
$AuCl_4^- + 3e^- \rightarrow Au + 4Cl^-$	0.99	$Mn^{2+} + 2e^- \rightarrow Mn$	−1.18
$NO_3^- + 4H^+ + 3e^- \rightarrow NO + 2H_2O$	0.96	$Al^{3+} + 3e^- \rightarrow Al$	−1.66
$ClO_2 + e^- \rightarrow ClO_2^-$	0.954	$H_2 + 2e^- \rightarrow 2H^-$	−2.23
$2Hg^{2+} + 2e^- \rightarrow Hg_2^{2+}$	0.91	$Mg^{2+} + 2e^- \rightarrow Mg$	−2.37
$Ag^+ + e^- \rightarrow Ag$	0.80	$La^{3+} + 3e^- \rightarrow La$	−2.37
$Hg_2^{2+} + 2e^- \rightarrow 2Hg$	0.80	$Na^+ + e^- \rightarrow Na$	−2.71
$Fe^{3+} + e^- \rightarrow Fe^{2+}$	0.77	$Ca^{2+} + 2e^- \rightarrow Ca$	−2.76
$O_2 + 2H^+ + 2e^- \rightarrow H_2O_2$	0.68	$Ba^{2+} + 2e^- \rightarrow Ba$	−2.90
$MnO_4^- + e^- \rightarrow MnO_4^{2-}$	0.56	$K^+ + e^- \rightarrow K$	−2.92
$I_2 + 2e^- \rightarrow 2I^-$	0.54	$Li^+ + e^- \rightarrow Li$	−3.05
$Cu^+ + e^- \rightarrow Cu$	0.52		

On the right-hand side of the arrow reactants are shown while on the left side are products of the electron transfer reaction. As we traverse the list from top to bottom, the potentials become gradually more positive which mean that it is easy to remove electrons from metals at the top than at the lower side of the list. For example, it is very difficult to oxidize Gold into its ion (Au^+). The voltage required for this is -1.83V, therefore Gold is called a noble metal.

Table 1.2 Standard reduction potentials for molecules with respect to SHE. The reactions are written for equimolar quantities of reactants and products to calculate the potentials for different molar ratios of reaction species, the Nernst equation can be employed. [63]

Half-reaction			*E*° (V)
Oxidant	⇌	**Reductant**	
$3Fe_2O_3(s) + 2H^+ + 2e^-$	⇌	$2\ Fe_3O_4(s) + H_2O$	+0.66
$Ag_2O(s) + 2H^+ + 2e^-$	⇌	$2Ag(s) + H_2O$	+1.17
$HClO(aq) + H^+ + 2e^-$	⇌	$Cl^-(aq) + H_2O$	+1.49
$SbO^+ + 2H^+ + 3e^-$	⇌	$Sb(s) + H_2O$	+0.20

When this principle is applied to concentration changes of oxidized and reduced entities contributing in electrochemical reactions, the resultant equation is called Nernst Equation.

$$E=E^0 + RT/nF.\ In\ (C_0/\ C_R) \qquad (1.3)$$

Where "RT/nF" denotes the gauge of energy (in the form of volts).

"n" is the number of electrons shifted during redox reaction.

"F" is the Faraday constant (overall charge/mole of electrons).

"C_O&C_R" are the concentration/activity of the oxidized and reduced species.

The exchange amid Joules/mole and volts comes from the explanation of electric potential with following equation;

$$-\Delta G^0 = nFE^0 \qquad (1.4)$$

Where "0" indicates the standard condition (For non-stoichiometric concentrations of species the Nernst equation is used)
"n" is the number of electrons relocated in each reaction and "F" is known as Faraday constant, the total charge for each mole of electrons (96,485 Coulombs).

1.6 Objectives

The main objectives of this research work carried out by us are as follows;

- Synthesis of thin, uniform and homogenous single NiO film on electrode grade carbon
- Enhancement in specific capacitance of bare carbon electrode material by increasing the number of electroactive sites participating in redox reaction at electrode-electrolyte interface
- Increase in specific surface area of thin oxide film by manipulating morphology of particulate film at micro/nano scale

Chapter 2

Literature Review

2.1 What are Supercapacitors?

Supercapacitors are basically electrochemical capacitors. They are also known as ultracapacitors or hybrid capacitors. This term is usually applied to energy storage devices based on the charge storage mechanism in the electrical double layer of very high surface area electrode in aqueous solutions [17]. These capacitors show superior capacitance than conventional capacitors due to higher energy density as well as power density along with cyclic efficiency [18]. Supercapacitors are recently focal area of research due to their fast charging mechanism [19].

The applications of supercapacitors. include microelectronics, transferable electronic devices, the distributed power generation devices and environment friendly hybrid vehicles. The conventions adopted for electrochemical capacitors are inherited from battery and fuel cells to define components of the device like anode, cathode and electrolytes. In case of ultracapacitors two high surface area electrodes are used called anode and cathode. If both electrodes are of same material, then they are known as symmetric capacitors. The efficiency of these capacitors can be enhanced by introducing a catalyst into the parent electrode surface like RuO2 (Ruthenium dioxide). The capacitors which utilize such catalyzed electrodes may be labeled supercapacitors. The use of such catalysts usually causes a reduction and oxidation (redox) couple reaction which is fast and reversible resulting in the higher capacitance as well as reduction of charging time. The second type of supercapacitors incorporates two different types of electrodes, for example a combination of nickel hydroxide (cathode/positive terminal) and carbon (anode/negative terminal) electrodes referred to as asymmetric capacitors. These capacitors are also termed as hybrid capacitors.

2.2 Types of supercapacitors

Supercapacitors are classified into two main categories, electrical double layer supercapacitors and pseudo-capacitors on the basis of their charge storage mechanism.

2.2.1 *Electrical double layer (EDL) supercapacitors*

These are so called because of the formation of electrical double layer in which charge separation takes place at the electrode-electrolyte interface under the influence of an applied Voltage. This voltage produces a current which is responsible for the separation of charges at electrode surface [20, 21] which is called non-faradaic.

2.2.2 *Configuration mechanism of Electrical Double Layer*

As soon as an electrode which is an electronic conductor is submerged into an aqueous solution which is an ionic conductor, the impulsive rearrangement of the charges takes place at the surface of electrode as well as in the aqueous ionic solution. separation of positive ·and negative charges result in the formation of electric double layer (EDL). The one layer exists inside the conductor surface and the other forms in the electrolyte at electrode-electrolyte contact area. This phenomenon is illustrated in Figure 2.1.

Figure 2.1 represents a simplified Helmholtz model for alignment of charges on both sides of the electrode surface. In part B of Figure 2.1 more details of the model are shown indicating the size of the cations and anions and their distance from the electrode surface. In Helmholtz model two planes known as Inner Helmholtz plane (IHP) and outer Helmholtz plane (OHP) are defined. The former represents the closest distance of the cations from the electrode surface while the latter expresses the nearest approach of the anions. The cations are larger in size than anions.

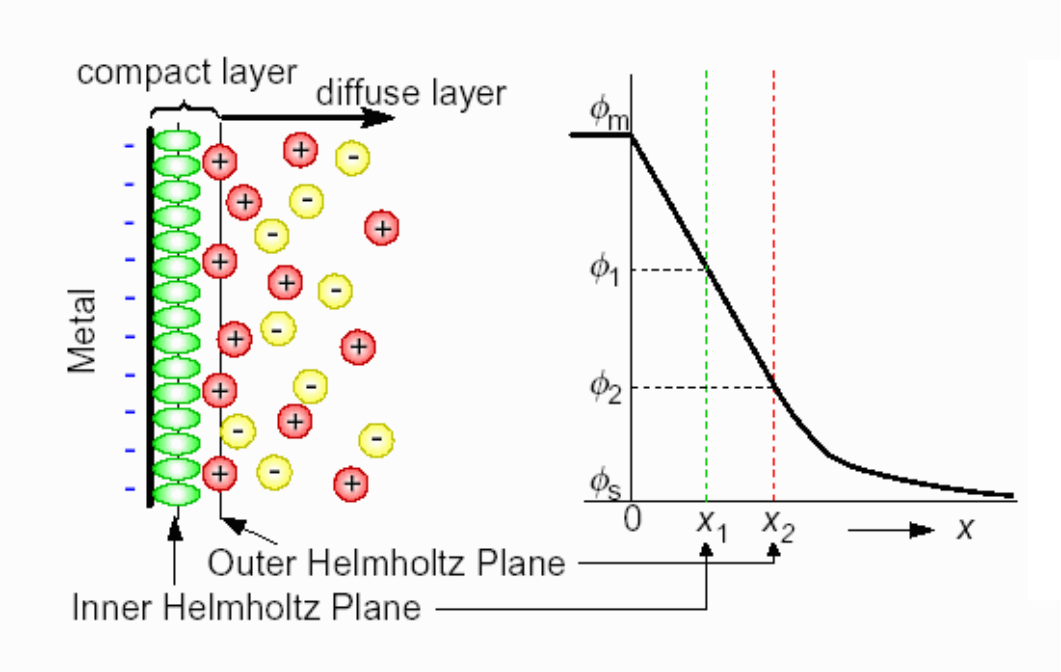

Figure 2.1. The double charged layer acts as a capacitive device consisting of charges in the electrolyte and inside the conductor surface distanced apart by the order of atomic dimensions. The properties of the EDL depend on many factors like surface morphology of the electrode, the chemical composition of the solution and electric field between the charges present at the electrode electrolyte interface. [17]

The cations are attracted towards the negative electrode surface by Coulombic forces. The electrostatic attraction of these ions present in the electrolyte towards electrode surface strongly depends on the chemical affinity of ions with electrode material as well as the charge strength of the electrical double layer. The double layer produces and diminishes in a very short time of about 10-8second which is called time constant of EDL. In this brief time interval, the double layer reacts to the applied potential changes. This phenomenon is attributed to charge re-alignment but not caused by any type of chemical reaction. This mechanism differentiates EDL capacitors from batteries and fuel cells where redox reaction takes place at electrode's surface.

It implies the slower time constant for redox reaction as compared to formation of EDL which is at the order of about 10^{-2}~10^{-4}sec. The delayed time is due to source of impedance arising from electrolyte and electronic circuit. However, the

redox reactions taking place at the electrodes impart capacitance known as polarization capacitance in the charge storage devices. When carbon electrodes are used in aqueous electrolytes, they possess 0 V charge versus standard hydrogen electrode. Under the influence of an external applied potential, the density of double layer increases by diffusion of more ions and electrons towards the electrode. This increased charge results in enhancement of capacitance(C) calculated as;

$$C = Q/V \quad (2.1)$$

Where, Q = amount of charge

V = applied voltage

Generally, carbon and metallic electrodes have an EDL capacitance varying between 10-40 µF/cm2.The capacitance value mainly depends on two key factors, the applied external potential and the contribution of IHP (Inner Helmholtz plane) in double layer. Conventional carbon electrode with large surface area has nearly a capacitance of 4F/g [17]. Currently, the nanoparticulate electrode materials are being explored to increase the surface area up to a level where high capacitance can be gained by more active participation of electrode material.

2.2.3 *Electronic Theory of Electrical Double Layer*

The electric field required for oxidation or reduction of molecules is only momentous within Debye length (l_d) or near to that from metallic electrode. The driving force to produce or neutralize the ions results from the free energy created by the electric field existing close to the electrode. The mechanism of charge transfer at electrode-ionic medium interface is depicted in Figure 2.2. When an ion leaves the electrode, and reaches at a distance which is greater than Debye length (l_d), it does not experience any inherent electr1c field. At this point the ionic movement in bulk solution is directed by the ascent of ion concentration. Typically, the one-dimensional term for evaluation of current density in any medium is given by:

$$Jn\,(x) = n(x)\mu_n \, d\Phi(x)/dx + kB\,T\,\mu_n \, dn(x)/dx \quad (2.2)$$

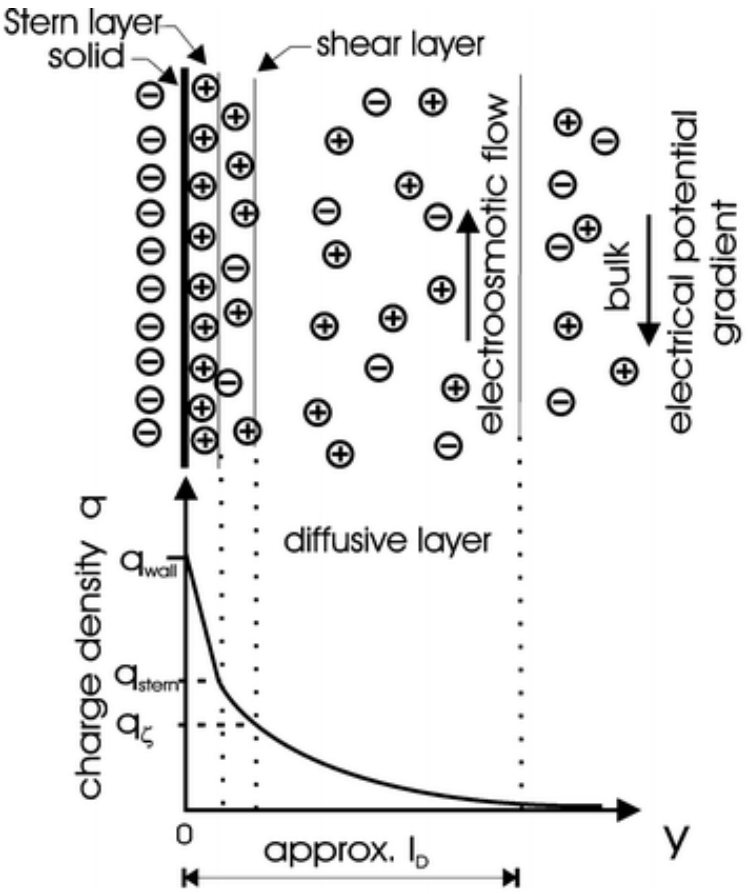

Figure 2.2 The basic concept of charge transmittance at metal-molecular medium interface. [15]

Where, the first expression of the above equation "$n(x)\mu_n$ dΦ(x)/dx" denotes the current inherited from the drift velocity of charge carriers having a density of *'n(x)" and* "μ_n" is mobility of these carriers within a medium of electric field "dΦ(x)/dx". This electric field has a negligible effed on the outer surface of double layer.

The second expression "kB T μ_n dn(x)/dx" illustrates the diffusion of ions (charged carriers) resulted due to entropy produced by concentration gradient of dn(x)/dx obeying the Fick's Law. The transportation of these charge carriers possess an associated electric field which is governed by Ohm's law. However, the driving force for current flow is entropy and is therefore temperature dependent. The net current crops up from the creation of ions at anode and their utilization at cathode resulting in a bulk diffusion of ions through the solution. This charge transfer mechanism is shown in Fig. 2.2.

2.2.4 *Mechanism of charge transfer between molecules*

Redox process is basically responsible for charge transfer between molecules. This process can be explained based on Kramer's theory. For example, look on simple reaction between ions of same nature:

$$Fe^{2+} + Fe^{3+} \longleftrightarrow Fe^{3+} + Fe^{2+}$$

The above reaction can be verified by spectroscopic studies. There is no net difference in free energy of reactants and products. The process is thermally activated and it can be described by Figure 2.3. This figure illustrates two different states, one of charged atom and the other a neutral atom. We are interested in understanding the electron transfer from one site to another site. The top portion of figure shows the reactant species and the bottom product species. The negatively charged ion is neutralized by environmental polarization shown by arrows around the ion in the figure. The polarization may be induced due to solvent or bond distortion or the mutual effect of both. This phenomenon is a consequence of accumulated free energy and causes a distortion of the medium from its original geometry, even in the absence of an electric field. This free energy is not sufficient for charge transfer, so external work is required to be performed. This work is known as reorganization energy for transfer of charge and is represented by "λ". If this energy is totally contributed by the solvent orientation, then it is named as solvent or outer shell reorganization energy. On the contrary, if bond distortion of the molecules is responsible for provision of this energy, then this type of principle is called inner shell reorganization energy. In general, these both types of phenomena occur during charge transfer process.

Marcus claimed that the energy required for shifting of electron from one atom to another atom depends on the level of environmental distortion and is quadratic in nature. In this way, he derived a simple equation to evaluate the activation energy for transfer of charge [20]. This expression for reactant atoms A & B as shown in the upper portion of Fig. 2.3 is given by;

$$E=1/2\ k\ (q- q_A)^2 \qquad (2.3)$$

Where "q" is, reaction coordinate and "q_A" represents the level of distortion along electron transfer path, when the electron lies on atom A. With the help of Marcus

equation, a graph can be drawn between electronic energy (of reactants as well as products) vs. reaction coordinate(q). The electronic energy which is shown on the vertical axis of graph is basically the addition of free energies of reactants, atom A with one electron resting on it and the atom B which is neutral. The horizontal axis represents the multidimensional reaction coordinate evaluated against electronic energy. As described by Marcus theory. the relationship is quadratic one following the Equation 2.4. The electronic energy is minimum at reaction coordinate "q_A" ·. A similar curve can be plotted for products including atom B with the possession of electron and atom A being neutral. In this case the free energy of products becomes minimum at "q_B" but with identical quadratic variation. The mathematical expression is given as:

$$E=1/2\ k\ (q- q_B)^{2} \qquad (2.4)$$

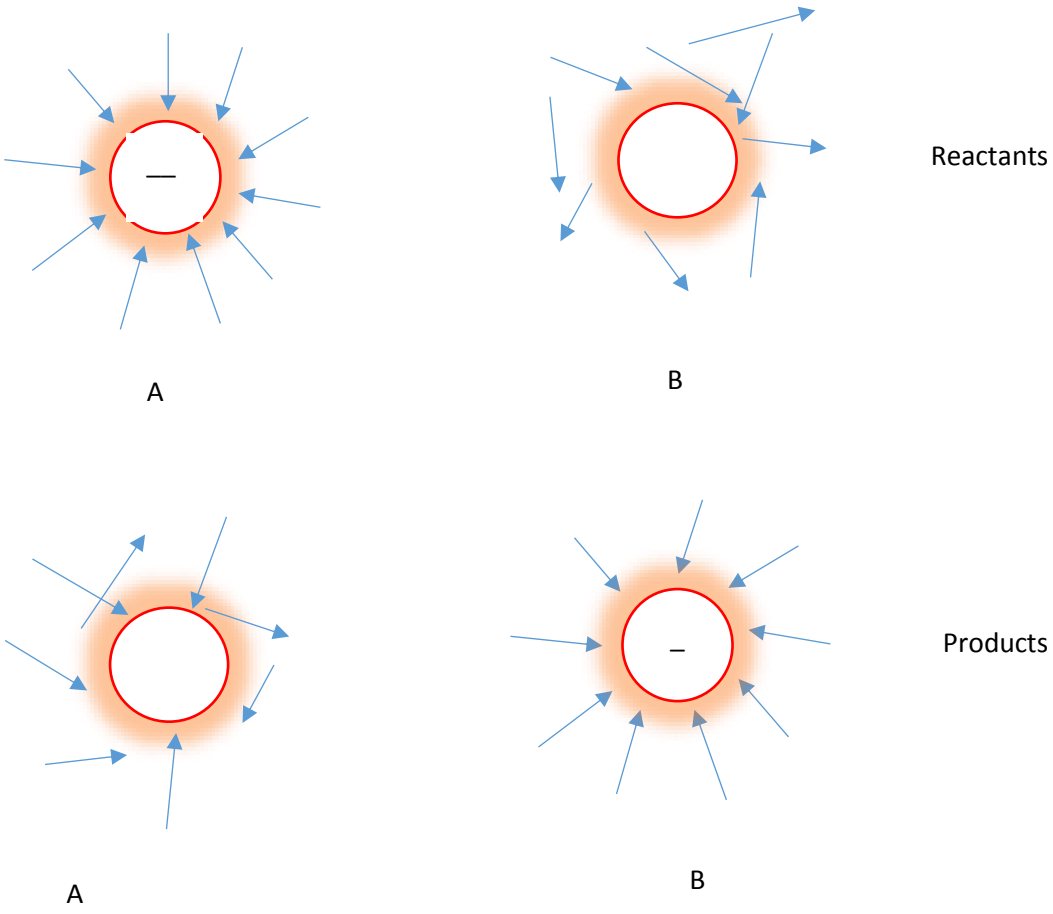

Figure 2 . 3 Theory of electron transition from one atom to another atom during charge transfer process between reactants and products (A& B atoms). [20]

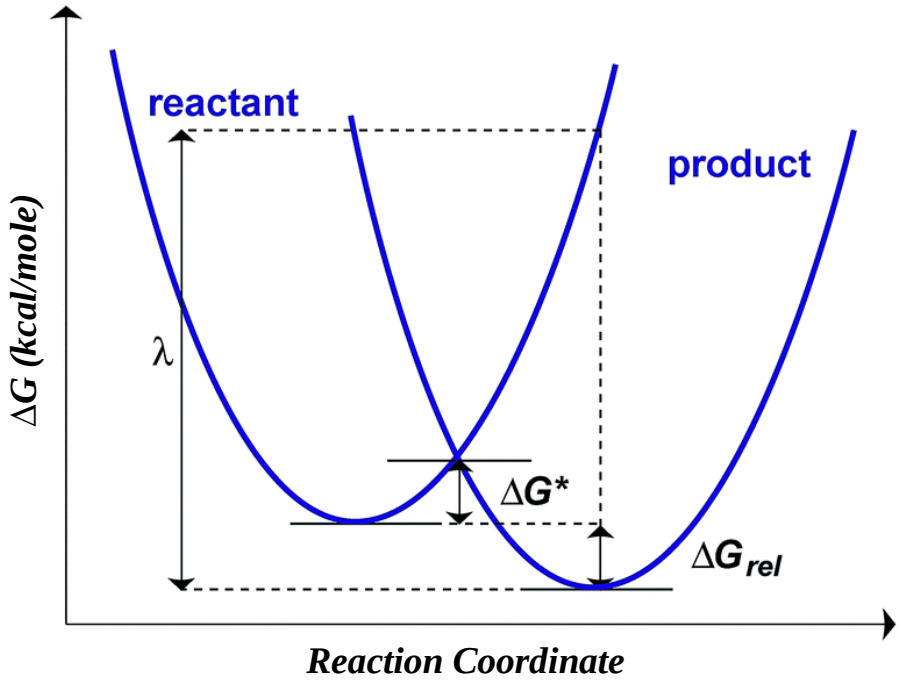

Fig. 2.4 The plot showing the correlation between net free energy of reactants as well as products vs. reaction coordinate (q). [20]

where “k” is spring constant which represents the warping of the potential surface. The mathematical equations describing the variation of electronic energy of both reactants and products with reaction coordinate “q" are plotted in Fig.2.4. This diagram gives us a clue about the reorganization energy " λ” which is to be provided when electron skips from atom A to atom B immediately as shown in the Figure by the upright arrow.

2.2.5 *Pseudocapacitors*

These are also called redox supercapacitors because the energy storage mechanism is attributed to the reduction and oxidation reaction (redox) which is rapid and reversible process that occurs at the electrode- electrolyte interface with change in oxidation number [17,21-22]. This charge storage mechanism is specifically known as pseudocpacitance and in contrast to conventional capacitor looks like a rechargeable battery.

2.3 Operational mechanism of EC supercapacitors

As mentioned above, supercapacitors have a close resemblance with batteries. The basic mechanism of EC capacitors can be explained by the following circuit;

C_a. Ri C_c

Where;

C_a = double layer capacitance of anode

C_C = double layer capacitance of cathode

Ri = internal resistance of electrochemical cell

Total capacitance of the cell can be calculated by the following equation;

$$1/C = 1//Ca + 1/Cc \quad (2.5)$$

In case of a supercapacitor, Ca = Cc

Therefore, total capacitance, C = 1/2 Ca

Today, the nanostructured electrode materials are most demanding due to their very high 2D surface area because it increases the wetting contact of the electrode with the electrolyte, electronic conductivity and electrochemical reactivity as well as reduction in cost. This makes the capacitance of supercapacitors in multiple orders of magnitude higher than conventional dry electrolytic devices. The maximum potential limit in case of EC capacitors with aqueous solutions is about 1V depending on the stability of the electrolyte. By using organic electrolytes, the voltage limit can reach up to 2.7V but at the cost of lower double layer capacitance and poor ionic conductivity. Energy storage of EC devices is computed by, $E= 1/2\ QV^2$, which indicates that the stability of organic electrolytes

at higher voltage permits the higher energy storage capability in capacitors.

Another disadvantage of organic electrolytes in the fact that their ionic resistivity is hundred times larger than aqueous electrolytes which results in slower response in the formation of electrical double layer under the applied current pulse. Therefore, the EC devices with organic electrolytes have slower charging speed.

2.4 Charge-Discharge mechanism of EC Capacitors

The charge-discharge behavior of symmetric EC capacitors having both similar electrodes of equal mass submerged in an aqueous or non-aqueous solution is depicted in Figure 2.5.

When no charge (Q) passes through the electrolyte, both electrodes of the capacitor are at the same voltage. In case of symmetric capacitor both electrodes are of the same material, therefore during charging potential of both the electrodes rises in the reverse directions. When one of the electrodes acquires a potential, which is equivalent to the stability limit of electrolyte, then the EC capacitor operates at its maximum voltage.

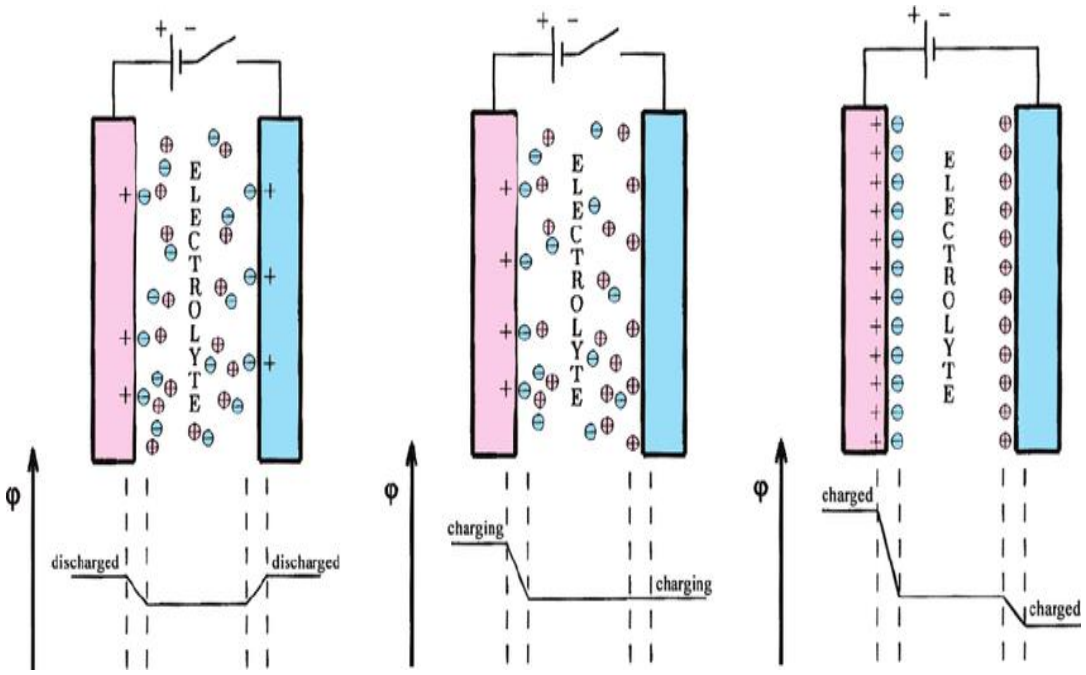

Fig. 2.5 Illustration of the charging behavior of a symmetric EC capacitor. [16]

In asymmetric capacitor, one of the electrodes is replaced by a battery electrode. The capacitance of' this electrode comes from famous redox reaction at the electrode electrolyte interface which is ten times higher than the conventional electrical double layer capacitance. As an example, if the carbon cathode in symmetric capacitor is replaced by a Ni $(OH)_2$ cathode, the capacitance of EC becomes double. This can be verified by substituting, $C_c = 10C_a$ in Equation 2.6.

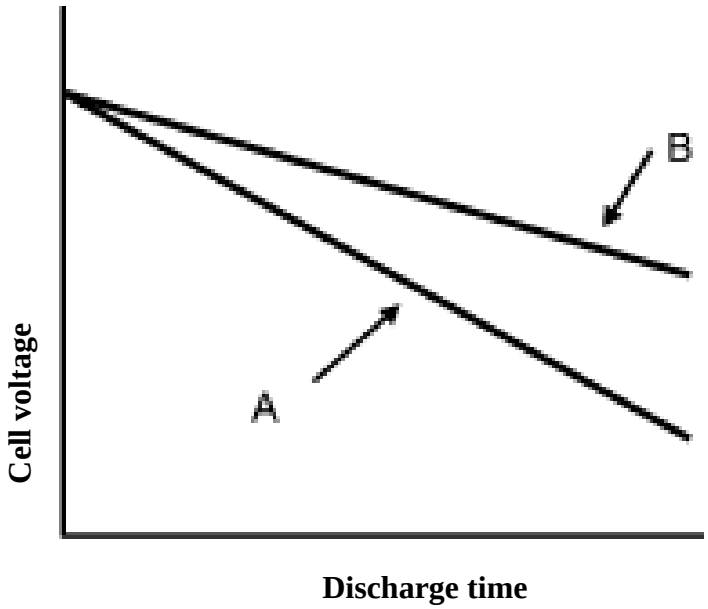

Figure 2.6 Typical discharge curve for hybrid capacitor: (A) for a symmetric capacitor and (B) for an asymmetric capacitor. [16]

$$1/C = 1/Ca + 1/10Ca \qquad (2.6)$$

$$C \sim Ca$$

This type of electrochemical capacitor is also known as hybrid capacitor. The characteristic discharge curve for such type of capacitor is illustrated in Figure 2.6. The capacitance of a battery electrode is much higher (3~10 times more) due to redox reaction than an electrode with a double layer capacitance which results in constant voltage of this electrode during charging and discharging process. So, the advantage of hybrid capacitor is that its voltage drops more slowly during discharge thus increasing its operational cycle.

To boost the kinetics and reversibility of redox electrodes during charge-discharge process, thin film electrodes have been prepared. Examples of such type of electrodes include Lithium inserted electrodes ($Li4Ti5O_{12}$), RuO_2 deposited on carbon, binary oxide (Mn-Ni oxide) films on graphite sheet [23]. nanostructured NiO on anodized alumina template [24] etc. All these thin film electrodes show 'pseudocapacitive' charge- discharge behavior during EC operation.

In our research work. we have deposited electrochemically NiO thin film on electrode grade carbon plate for use in electrochemical capacitors to improve energy capacity of electrodes and enhance active surface area at submicron level.

2.5 Electrode materials for Supercapacitors

Various types of inorganic as well a s organic materials have been used as electrode materials for supercapacitors to enhance the energy and power density of energy storage devices.

2.5.1 *Organic materials*

In the category of organic materials, conducting polymers have also been utilized as electrode materials for supercapacitors [25]. For example, when polyacetylene, molecular formula (..... $CH_2CH_2CH_2$....) is doped with oxidizing or reducing agent. it shows the reasonably good conductance~ $10^3(\Omega\text{-cm})^{-1}$ [26]. Other example is oxidation of polypyrrole with high quantity of oxidizing agent. A variety of oxidizing agents which can be used for doping of conducting polymers include Iodine, $AsCl_5$ and $FeCl_3$. The conducting polymers can be visualized as molecular wires which transport electrons through nano particles, fibers or filaments. Polyaniline when synthesized in crystalline form shows metallic behavior.

2.5.2 *Inorganic materials*

Previously various inorganic materials were considered among good candidates for supercapacitor electrode material in which most prominent was hydrated ruthenium oxide (RuO_2) with reasonably good capacitance but could not be well commercialized due to its higher cost [27, 28].Therefore the current research is

concentrated on the low cost earth abundant transition metal oxides like NiO [29], $Ni(OH)_2$[30],MnO_2(31],Co_3O_4[32] and V_2O_5[33].

2.5.3 *Carbonaceous materials*

3D carbon is the oldest and well commercialized material being used as an electrode in dry batteries and capacitors. Currently the graphene which is a single layer of carbon atoms and building block of graphite has found potential applications in supercapacitors due to its excellent electronic conductivity and good capacitance [34]. Also, the graphene can be synthesized at a reasonable cost. Recently, the Graphene Oxide (GO) is functionalized with LOF covalently and its behavior is studied as a supercapacitor electrode material and it showed four times increase in capacitance as compared to GO [35].

2.6 Nickel Oxide

It is a semiconducting material with good specific capacitance characteristics for use in energy storage devices. Pure Ni metal lies. in the group of transition metals with variable oxidation state ranging from +2 ~ +4 in various nickel compounds. Among nickel oxides Ni (II) oxide (NiO) is investigated thoroughly. Other nickel oxides e.g. Ni (III) oxide(Ni_2O_3) and Ni(IV) oxide(NiO_2) have been synthesized but not very well described [36]. The mineral form of NiO is found infrequent and named as Bunsinite.

The non-stoichiometric Ni_2O_3 is the nickel oxide in black color while stoichiometric NiO is green in color. This color change is attributed to the variation of Ni: O ratio from 1:1. The traces of Ni_2O_3 are found on the metallic nickel and during nickel oxidation as an intermediate compound [37]. Nickel hydroxide has also been synthesized and used for oxidation of alcohol to benzoic acid. Nickel oxide assumes the sodium chloride structure named as rock salt structure. This is a p-type semiconductor [38] having a band gap of 3.6-4.0 eV and conduction energy of 1.8eV. The interest in NiO arose owing to its good properties like. chemical stability and complimentary optical, electrical, magnetic and catalytic properties. Present1y NiO and its submicron/nano-scaled particles are being used in multiple applications including supercapacitor electrodes, super magnetic materials, transparent conducting films, gas sensors, catalysis, lithium ion battery electrodes, dye sensitized solar cells,

SOFC anodes [39,40,41], electrochromic devices [42], photo electrolysis [43]. Nickel Oxides have high electrochemical reaction activity [44] which makes them suitable for supercapacitor applications. Nickel oxide has a high theoretical specific capacitance of 3228F/g [45].

The current research is focused on synthesis of NiO film through various synthesis routes like chemical. precipitation [46], sol gel process, electrophoresis and electrodeposition is still far from its theoretical capacitance. Therefore still there is a need to enhance the specific capacitance of NiO through various strategies by enhancing the active utilization of the NiO matrix. The capacitance of NiO depends on. applied potential in a potential window of nearly 0.5V thus making it appropriate as a positive electrode in energy storage devices. However, its use as a negative electrode will result in a narrow potential window [47].

In short, NiO is economical than RuO_2 and environmentally benevolent and is well suited for processing by a variety of techniques that makes it a material of choice for future highly efficient electrochemical supercapacitors. [48, 49].

2.7 Pourbaix diagrams and thermodynamic stability

Pourbaix diagram is also called potential-pH diagram. This diagram provides information about the probable equilibrium phases existing in an aqueous system resembling like a phase diagram. The horizontal axis shows the pH value and the vertical axis denotes the potential in volts against the standard hydrogen electrode (SHE) potential. The potential value is computed by using Nemst equation. The lines of the diagram indicate the co-existence of the equilibrium phases present on either side of the line. Pourbaix diagram gives information about the stability of a metal in certain regions at a given pH-potential. The three main regions defined by the Pourbaix diagram are corrosion, immunity and passivation. Passive region shows the conditions at which some type of protective coating is formed on the metal surface. These diagrams are drawn at constant temperature and solution composition. The diagrams can be rebuilt for other temperatures and solution compositions by using software. As an example, the Pourbaix diagrams of Mn and Ni whose oxides are important electrode materials for supercapacitors have been illustrated in Figure 2.7 and 2.8 respectively. These diagrams present the formation of different phases at a

potential versus the pH value of the aqueous solution. With the help of these diagrams, it can be assessed that what potential should be applied to the electrode and how much should be the pH value of electrolyte medium to deposit electrochemically metallic Mn or Ru and their oxides through galvanic cell. For example, RuO_2 can be deposited above 0.5V applied potential for all pH values of the electrolyte. Higher oxidation states of Cobalt [+3 and +4] can be achieved at relatively higher potentials [50].

Earth abundant transition metal oxides demonstrate the characteristic of variable oxidation states. However, during electrodeposition transition to multiple oxidation states may cause the formation of soluble species resulting in the material removal from electrode [51]. This fact causes the degradation of electrode material and negative effect on its stability. One example of this is Manganese Oxide in which Mn (VII) is soluble and in minute quantity lowers the efficiency of electrode. During redox reaction it may precipitate again after further reduction and probably deposit on the cell parts. On the contrary, it can deposit on the electrode again with less favorable crystallographic orientation [51] thus resulting in low activity during redox cycle.

The Pourbaix diagram of the nickel is shown in Fig 2.8 which depicts that up to an applied potential of about -0.75V, metallic Nickel may be electrodeposited in acidic as well as alkaline aqueous electrolyte. In addition to this, the diagram shows that solid nickel is stable in a wide range of pH values of electrolyte medium. Oxidation state of nickel varies between +2~+4 depending on the applied potential and pH value of the aqueous solution. It means that nickel as an anode material shows good stability in aqueous solutions. Due to its comparatively low cost and high stability, nickel oxide is considered as an excellent material for electrodes of supercapacitors.

From the Fig 2.8, it is also clear that to deposit NiO directly on electrode the electrolyte should have high alkalinity with pH value greater than 9 and an applied potential of > -0.5V.

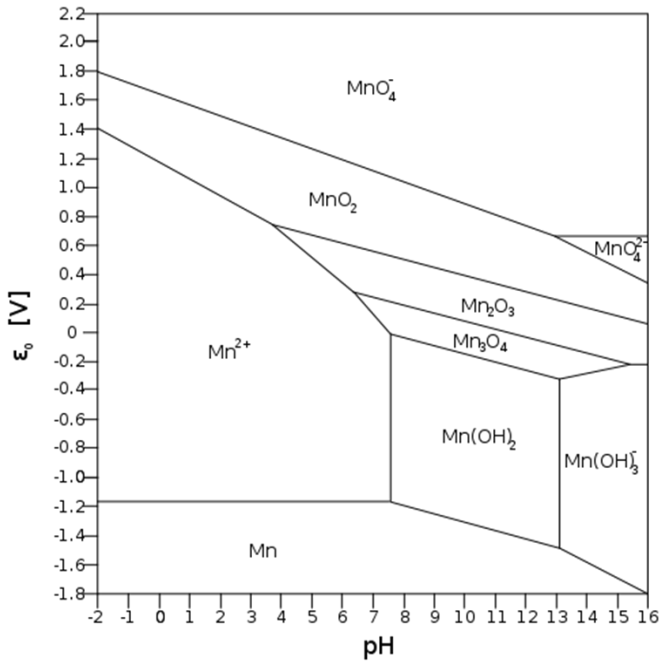

Figure 2.7 Pourbaix diagram of manganese(Mn). [50]

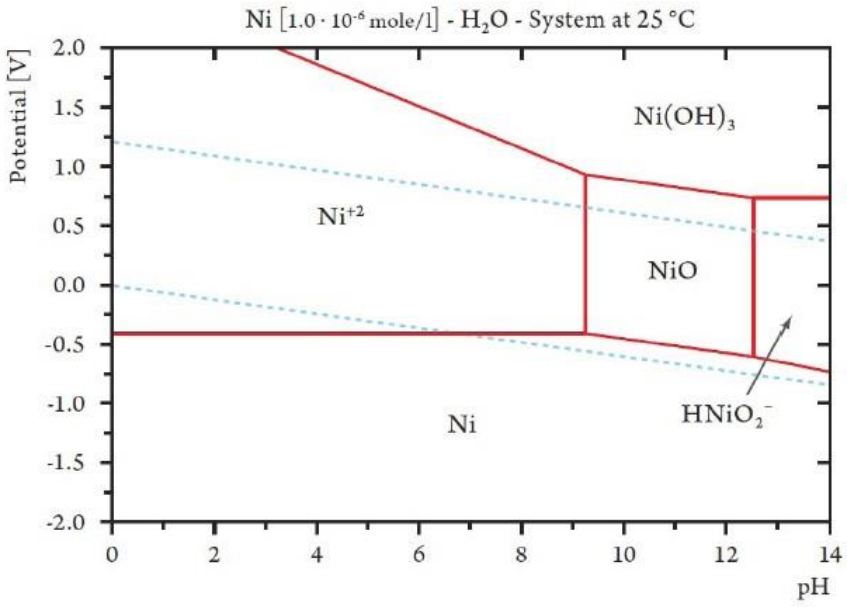

Figure: 2.8 Pourbaix diagram of Nickel. [50]

2.8 Mechanical Stability of Oxide materials

Mechanical stability of oxide with the substrate is very vital for efficient performance of electrode material. For example, in case of cobalt, the oxidation state varies from +2~+4 but its coordination geometry does not change resulting in the structural stability of electrode material [50]. Stability of electrode material also depends on the synthesis route. High temperature promotes the development of crystalline materials but on the contrary the low temperature synthesis favors the production of amorphous films. Crystalline structures are more stable mechanically than amorphous ones due to less defected structure. The reason is that with crystallinity the lattice structure becomes more ordered and its potential to absorb the lattice strain is much better than amorphous material [52].

2.9 Synthesis of Nickel Oxide

NiO can be synthesized by utilizing different techniques listed below;

- Thermal decomposition method [53]
- Evaporation through electron beam [54]
- Anodic electrochemical deposition [55]
- Cathodic electrochemical deposition [42]
- Sol- Gel method [56]
- Electrophoresis

In the present research work, the NiO is synthesized by cathodic electrochemical deposition process. Electrochemical deposition process is a simple, low cost. versatile and accurate process for deposition of thin oxide films. The process is carried out at room temperature thus making it commercially viable on large scale. In the following section the basic mechanism of this process along with its brief history will be described.

2.10 What is electrochemical deposition?

In electrochemical deposition process, the metallic ionic species present in an aqueous electrolyte are reduced by redox reaction on a conductive surface through an applied electric current or potential in a galvanic cell. By this technique, micron as well as even submicron thick uniform films of metals and their oxides can be synthesized. In Figure 2.9, the basic components of an electrochemical cell are shown.

2.10.1 Brief history and advantages of electrochemical deposition

Electrochemical deposition was initiated in 1800 by Volta. He provided current to an electrochemical cell from an external source and deposited material on an electrode. Before the advent of electrodeposition, electroless technique was employed for deposition of metals without use of any current. Basically two schemes are used in electroless technique. One method is called replacement plating in which two metals with different electrode potentials are deposited on each other e.g. gold has higher electrode potential than copper and hence can be deposited on copper surface.

The alternative method used for electroplating is carried out through the use of a reducing agent. The process was discovered in 1940s by two scientists Grace Riddell & Abner. The source of electron was a chemical reducing agent. The dissolved metal ions in the aqueous solution consumed these electrons for reduction to atomic form. The research and development in the field of electroless deposition is still going on [57].

Electrochemical deposition flourished significantly with the advent of efficient electrolytes for precious metals including Au and Ag. Specifically, Electroplating industry took a lot of benefit from this technique. The requirement of cyanide based baths remained a major disadvantage of electroplating process due to their toxicity. Therefore, it was a big challenge to find suitable alternative electrolyte baths for electrodeposition which are environmentally benign.

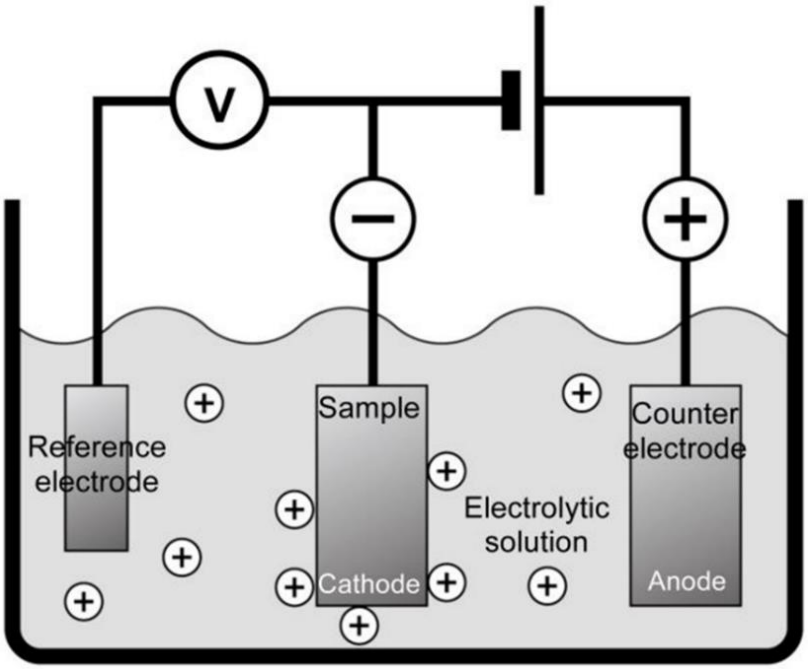

Figure 2.9 Schematic of electrodeposition technique. [42]

Previously the efforts were made to have a basic understanding of the electrodeposition process. Regarding this Tafel interpreted that the relationship between applied potential and deposition current during electrochemical reaction was linear using the concepts of statistical thermodynamics. After nucleation of metallic ions on substrate, the growth of metal atoms to form layers on the electrode was explained in the light of screw dislocation by Kaischew and Budevski in 1960.The experimental work required for understanding of the electrodeposition process at atomic level remained infeasible due to deficiency of an appropriate facility which can be employed in the existence of an elect1olyte. Therefore the deposited surface should be examined after taking away from electrolyte solution. After a long lime, the invention of STM has made achievable the in-situ inspection of electrodeposition in galvanic cells. This was marked as an innovative step in the modeling of electrodeposition process due to high resolution surface probe. Presently it has made possible not only the surface imaging but also the treatment of atoms to deposit them at predestined locations [58].

One of the major advantages of electrodeposition process lies in its capability to produce 3D geometrical structures. In addition to these thin films even at nanometer

regime can be formed and it is well established that nano-structures enhance the active utilization of the electrode surface [59]. The process is economical and can be accomplished at very low potential and current values. It is versatile and can be applied to modify various types of surfaces as well. The applications of electrodeposition process envisage various areas including ornamental, surface engineering, micro and nanoelectronics, biomedical, energy production and energy storage sectors.

2.10.2 Configuration of electrode systems in electrochemical deposition

Two electrode as well as standard three electrode galvanic cells are used for electrochemical deposition on the working electrode.

2.10.3 Design of two electrodes system

In this design, counter electrode is used to gauge the potential difference between working electrode and electrolyte. In two electrode system, the voltage of the counter electrode remains constant during operation of the cell. Therefore, any minute potential drop in the cell with time results in the change of interfacial potential of the working electrode. However, if magnitude of current becomes very high then potential of the counter electrode changes, to overcome this situation three electrodes galvanic cell has been designed. Following properties are required for the electrode to qualify as a counter electrode (CE);

- High speed electron transfer kinetics
- High surface area to minimize the current density
- To keep constant concentration of electrolyte species during current flow in redox reaction.

2.10.4 Design of three electrodes system

In this system, the potential of the working electrode is determined against the reference electrode. During operation of galvanic cell, current flows between working electrode and counter electrode. Very minor current passes through the reference electrode with the help of impedance operational amplifier. Therefore small sized polarizable electrodes can be used as reference electrodes. Potential of reference electrode changes with temperature minutely e.g. per degree

increase in temperature causes the potential to differentiate between 0 .5~ 1 mV. Actual potential of any electrode is calculated by Nemst equation which is implied from standard electrode potential and concentrations of species taking part in redox reaction.

$$E = E^0 + RT/nFIn1/[Cl^{-1}] \quad (2.7)$$

Where,

E^0 = standard electrode potential

E =interfacial potential of the electrode in bulk solution

R =Universal gas constant

T =Absolute temperature

n= valence of the element

F=Faraday's constant

Cl^{-1} =activity of chloride ions in Ag/AgCl RE

2.10.5 Electrodeposition techniques

Electrodeposition techniques are classified based on whether cathode or anode is used as a working electrode. The required material is deposited on the working electrode.

2.10.6 Cathodic electrodeposition

The positive electrode at which reduction takes place is called cathode. The deposition of metals as well as their oxides during metal extraction processes and electrolysis takes place on the cathode [42]. Cathode is provided negative voltage or current during the electrochemical cell operation.

2.10.7 Anodic electrodeposition

In this technique metal, oxides are deposited on the negative electrode of electrochemical cell called anode where oxidation takes place during electrolysis. At anode, metallic species can't be deposited because reduction reaction does not take place. By using this method both single metal oxides [42] as well as binary metal oxides [60] are electrodeposited on the working electrode.

2.10.8 Synthesis mechanism of NiO electrodeposition

The electrodeposition of NiO on the working electrode gets the benefit of $Ni(OH)_2$ precipitation principle by following reactions:

$$Ni^{2+} + 2OH^{-1} \longrightarrow Ni(OH)_2 \quad (1)$$

The produced $Ni(OH)_2$ reacts with hydroxyl ions of aqueous electrolyte according to the following equations to form NiO_2 [61]:

$$Ni(OH)_2 + OH^- \longrightarrow NiO\text{-}OH + H_2O + e \quad (2)$$

$$NiO\text{-}OH + OH^- \longrightarrow NiO_2 + H_2O + e \quad (3)$$

The overall reaction for the electrochemical deposition of NiO_2 in an aqueous solution., having Nickel ions (Ni^{2+}) can be rewritten as:

$$Ni(OH)_2 + 2\,OH^- \longrightarrow NiO_2 + 2\,H_2O + 2\,e^- \quad (4)$$

Chapter 3
Characterization Methods

3.1 Voltametric techniques

The response of current (I) is studied under the influence of applied potential (E). In this method. An external potential is provided to working electrode and the current generated due.to this potential is measured when it passes through the electrochemical cell. Further by changing the applied potential, the change in current is measured after a time interval (t). Depending on the applied potential. The cations and anions present in the electrolyte go through oxidation or reduction reaction at electrode electrolyte interface.

Voltammetry is performed by using the following basic parts;

- Working electrode (Electrode material to be analyzed)
- Reference electrode
- Counter electrode
- Ionic Electrolyte

There is a vast range of Voltametric techniques employed based on specific requirements of the work including cyclic voltammetry (CV), linear sweep voltammetry (LSV), chronoamperometry(CA), chronopotentiometry(CP), staircase voltammetry, square wave voltammetry etc. Regarding our project work, we are interested specifically in CV.

3.1.1 Cyclic voltammetry (CV)

Practically the cyclic voltammetry is performed under nonequilibrium conditions to measure the current with respect to applied potential. The potential of the

experimental electrode is swept with respect to reference electrode with the help of an electronic circuit. The current is measured passing through the experimental electrode during this process. By keeping all the other parameters constant, the current recorded is found to be maximum when just half of the quantity of ions existing in the solution is reduced and the remaining half is oxidized. The critical potential at which this phenomenon occurs is known as formal potential. As the potential becomes more negative, the number of reduced ions increases and conversely the oxidized ions become lesser in the solution. Below the formal potential, the current rises again because the number of ions potentially available for oxidation becomes abundant. On the contrary, when formal potential is crossed towards positive side of external potential, the oxidation current drops even though rate of oxidation process rises. The reason is that the quantity of ions still accessible for oxidation reduces. This type of measured current versus potential cycle is illustrated in Figure 3.1. This specific cyclic voltammogram (CV) Is observed for an electrode possessing a thin molecular film of Fe atoms existing in two oxidation states namely Fe^{+2} and Fe^{+3} ions. The containment of ions in this film eradicates the requirement for mobility of ions to the surface of electrode through diffusion. The upper peak in the CV diagram represents the maximum current which is produced when just half of the population of ions in the solution is oxidized to Fe^{+3} oxidation state. As the applied potential is further increased, the current falls with the oxidation of remaining ions. The bottom peak in CV occurs when the potential is reversed at a stage when accurately half of the oxidized ions are reduced to Fe^{+2} ions. Finally, the current again drops because the number of oxidized ions available for reduction becomes low. Both the upward and downward peaks occur almost at the same position which shows that this process is reversible. The symmetry of this CV curve results since Fe^{+2}/ Fe^{+3} ions are already tied up with the surface of the electrode through the thin film which prevents time delays involved in transport of ions from the bulk solution to the surface through diffusion. The analysis of additional intricate CVs, dealing with dissolved ions, is presented in detail elsewhere [62].

The applied potential is altered in cyclic shape at a fixed scan rate in a narrow potential window (say E1-E2). At a predetermined scan rate, the scan is performed

in both forward and reverse direction. The current produced is recorded as a function of applied potential. In case of cathodic scan, the potential declines and current is negative. Alternatively, in case of anodic scan, the potential raises with time and current is positive. The potential is manipulated at working electrode with respect to reference electrode. The resulting current is determined at counter electrode. In addition to other electrochemical properties, the specific capacitance of an electrode material can be measured by using this wonderful technique. The stability of an electrode during charge discharge cycles can also be assessed by CV [63-65].

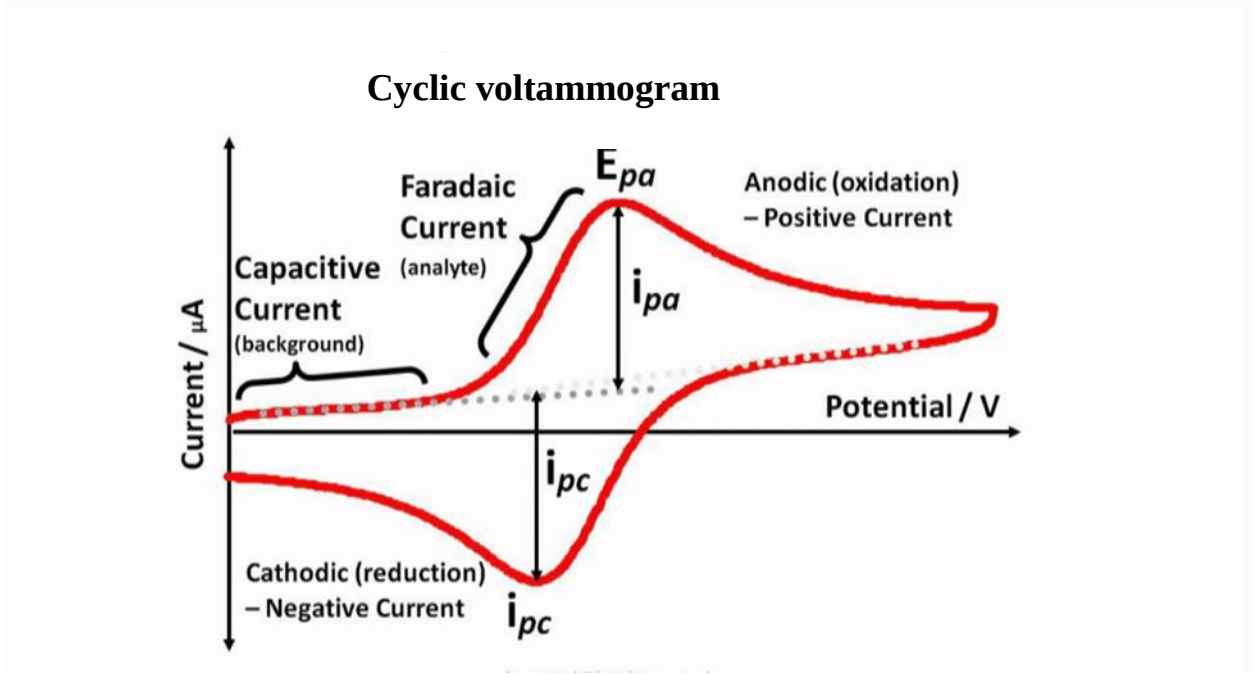

Figure 3.1 Cyclic voltammogram [63]

3.1.2 Calculation of specific capacitance through CV

With the help of cyclic voltammetry, the specific capacitance can be assessed by different methods;

Method I

In this method, the specific capacitance(C) of electrode material is calculated with the assistance of cyclic voltammogram which is recorded through a definite potential limit versus a reference electrode. The following mathematical equation is used

for this purpose:

$$C = dQ/dV = I/(dV/dt)$$

Where, Q= charge on the electrode

V=Potential

I=average current

dV/dt =voltage scanning rate

Finally, the specific capacitance of the electrodeposited electrode is obtained by dividing the capacitance by its respective weight.

Method II

By making use of Galvanostatic discharge curves obtained by applying a certain current density to the electrode film in aqueous alkaline electrolyte through a fixed potential window. Potential drop is measured at different current densities with respect to time. The specific capacitance of electrode (C) is evaluated by using the following relation [66];

$$C = Ixt/(Vxm)$$

Where, I=Discharging current

t=discharging time t

V= potential drop (IR) during discharge

m=mass of deposited film

Method III

The specific capacitance can be calculated by using the EIS analysis. The following equation is used based on the results of Nyquist plot employing the low frequency data;

$$Z'' = (2\pi f C)^{-1}$$

Where, Z" = imaginary part of the impedance

f = frequency

C=capacitance

3.2 Scanning Electron Microscope (SEM)

Electron microscope is a highly useful characterization tool for getting information about morphology, surface topography, phase differences, chemical composition and crystal structure of the sample. Electron gun is the source of electron beam which is focused on the sample. The combination of condenser and objective lenses directs and focuses the electron beam on the specimen. This focused beam spots on the surface of the sample and interacts with a certain volume of the sample. The electrons interact with the sample elastically or inelastically. Elastic interactions result in the form of back scattered electrons(BSE). This type of signal provides useful information about the compositional differences in the material because the phases with high value of atomic number(Z)appear bright as compared to the phases with low value of Z. In contrary to this, the inelastic interactions of the electron beam with the sample produce secondary electrons (SE) out of the specimen. lit case of secondary electrons, only those electrons are detected which are generated near the surface because they can get away easily.

This type of signal is more responsive to the surface of the sample as compared to its atomic number (Z) [67]. The secondary electrons offer high resolution image of the object as compared to their counter parts due to smaller sampling volume. These signals generated from the sample are detected by specific detectors known as BSE and SE detectors. Amplifiers are used to enhance the signal strength resulting in an enlarged image. Image quality is improved by altering the potential of the sample surface. The reason is obvious that in the charged area more secondary electrons escape as compared to the adjacent area that is reflected in black and white image.

We used JEOL scanning electron microscope (JSM 6490LA) for micro-structural characterization of our samples in this research project.

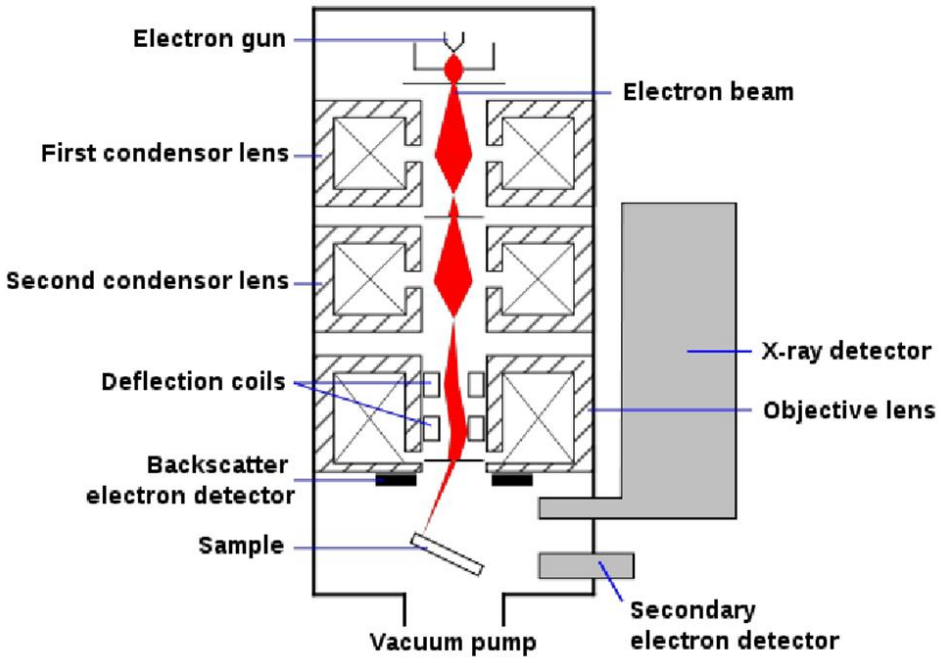

Figure 3.2 Schematic diagram of SEM [67]

3.3 X-Ray Diffractometer (XRD)

This characterization tool is used for identification of elements and their compounds as well as to resolve the crystal structure and lattice constants of a crystalline material. The governing principle of this machine is that when X-rays strike on the crystalline specimen at definite angles, the diffraction of beam occurs. These diffracted X-ray beams interact with each other to augment or annul the effect of each other. The constructive interference takes place where the diffracted rays are in phase and the destructive interference occurs where the rays are out of phase [68]. The famous scientist Bragg defined the conditions under which constructive interference takes place when X-rays are reflected from a set of parallel lattice planes. Bragg's Law classifies the incident angle of X-rays in relation to crystallographic lattice planes at which diffraction peak will arise. As per Bragg's relation constructive interference will be obtained when path difference is an integral number (n) of X-rays wavelength (λ).

Mathematically.it can be described as;

$$n \lambda = 2d \, Sin\Theta$$

Where,

Θ = incident angle of X-ray beam, d= interplanar spacing, n=order of diffraction, λ =wavelength of X-rays

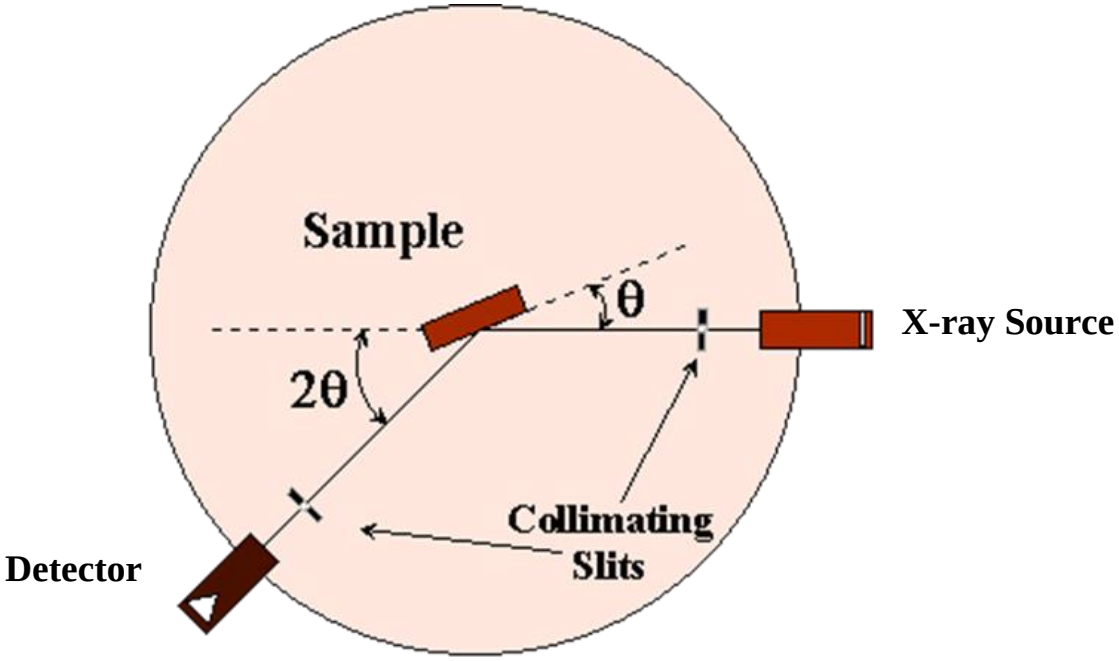

Figure 3.3 Schematic diagram of XRD [68]

Regarding this project work, the XRD patterns of the samples were acquired by using x-ray Diffractometer (Model STOE Θ - Θ).

Chapter 4

Experimental Work

4.1 Materials

The entire chemicals used for synthesis of thin films and cleaning of substrates were of analytical reagent grade. The materials were used as purchased without any further treatment. Nickel (II) Nitrate hexahydrate [$Ni(NO_3)_2.6H_2O$], Boric Acid (H_3BO_3), Potassium Chloride(KCI) and Potassium hydroxide (KOH) were utilized in different procedures. Commercial grade Sulfuric acid and Ethanol were applied to remove the surface contamination and defects of substrates. Electrode grade carbon plate, purchased from China was used as a substrate.

4.2 Preparation of NiO thin films

Thin films of Nickel Oxide were synthesized by electrochemical deposition method. A two-step strategy was adopted for formation of NiO thin films;

1. Direct electrodeposition of Ni/NiO and $Ni(OH)_2$ on carbon substrate.
2. Initially electrodeposited film was annealed at 250 ^oC in air to transform any residual metallic Ni as well as $Ni(OH)_2$ completely into NiO.

4.2.1 Electrochemical Deposition of Ni/Nickel Oxide

Aqueous electrolyte of Nickel (II) Nitrate hexahydrate was used for synthesis of NiO thin film on electrode grade carbon plate through three electrodes standard galvanic cell.

4.2.2 Chemical Composition of Bath

- 0.14M Nickel (II) Nitrate hexahydrate [$Ni(NO_3)_2.6H_2O$]
- Deionized water (with a resistance of $\geq 18M\Omega$).
- 0.1 M Potassium Chloride(KCI) as supporting electrolyte
- Boric acid (H_3BO_3) as pH buffer.

The process of electrodeposition was performed at ambient temperature.

4.2.3 Preparation of substrate

The surface cleaning of substrate is very vital for quality electrodeposition of any species. Electrode grade carbon plate was used as a substrate/ Working Electrode (WE) containing an electrical resistance of 8.5μohm and a density of ~1.70g/cm^3. Prior to employing as working electrode, it was polished with SiC paper (200. 800 &1000) to a rough surface finish. Then it was etched in 20wt% H_2SO_4 solution at room temperature for 20sec. After etching. the substrate was dipped into 2M methanol solution again for 20sec to remove any macro level surface defects and contamination. After chemical cleaning, the sample was washed in double distilled water. Finally, the specimen was dried in oven at 65 °C for 06hrs.Finally the specimen was insulated with Silicon sealant to expose a standard surface area of 10x10 mm^2 for deposition as a working electrode in standard three electrodes galvanic cell.

4.2.4 Preparation of Chemical Bath

The precursor AR grade Nickel (II) Nitrate hexahydrate which was purchased from Sigma Aldrich, has been dissolved in DMW (demineralized water) having a resistance of ≥ 18MΩ, to form aqueous electrolyte bath. The solution was stirred magnetically for 15 minutes to ensure uniform dissolution. The concentration of aqueous solution was maintained at 0. l5M. To make 250 ml of solution, Molarity was calculated by using the following formula;

Molarity (M) = Mass of solute/ [Molar mass of solute x l / vol. of solution (dm^3)]

Where, $1dm^3$ = 1 liter

Figure 4.1 As prepared 0.15 M Nickel (II) Nitrate hexahydrate [$Ni(NO_3)_2.6H_2O$] aqueous solution

The pH of the solution was preserved at -4 by using boric acid(H_3BO_3) as a pH buffer. The green color solution is shown in Figure 4.1. The bath was maintained at room temperature during electrodeposition.

4.2.5 Configuration/Design of Electrode system for electrodeposition

Nickel oxide/hydroxide was electrodeposited on the carbon substrate in a standard three electrode galvanic cell. The graphite rod was used as a counter electrode and reference electrode employed was SCE (saturated calomel electrode). The experimental set up is elaborated in Figure 4.2.

A constant current of -2.1mA vs. SCE (reference elec1rode) was applied in Galvano static mode as well as using a constant potential of -0.9 V vs. SCE in Potentiostatic mode by using a computer controlled Potentiostat during the electrodeposition process. Entire experiments were conducted using GAMRY Reference 750 Galvanostat /39 Potentiostat.

The recorded Galvanostatic and Potentiostatic curves during electrodeposition process are shown in Figures 4.3 and 4.4 respectively.

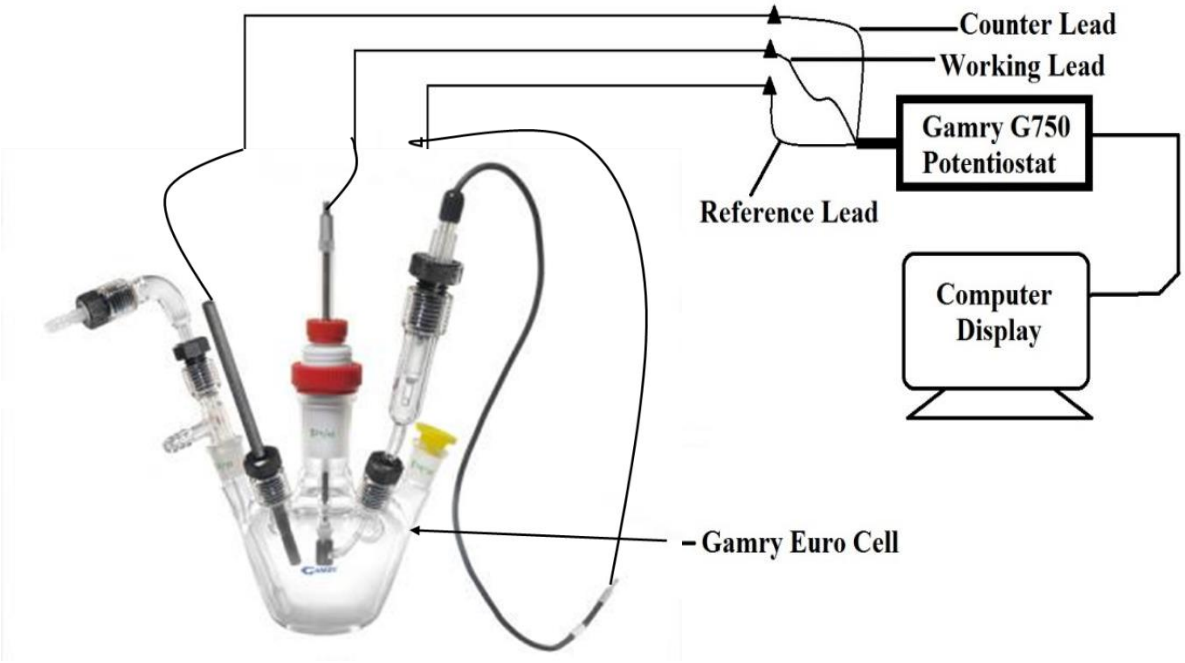

Figure 4.2. The experimental set up for electrodeposition process

As synthesized electrodeposited films are shown in Figure 4.5. The detailed experimental parameters are listed in Tables 4.1 and 4.2.

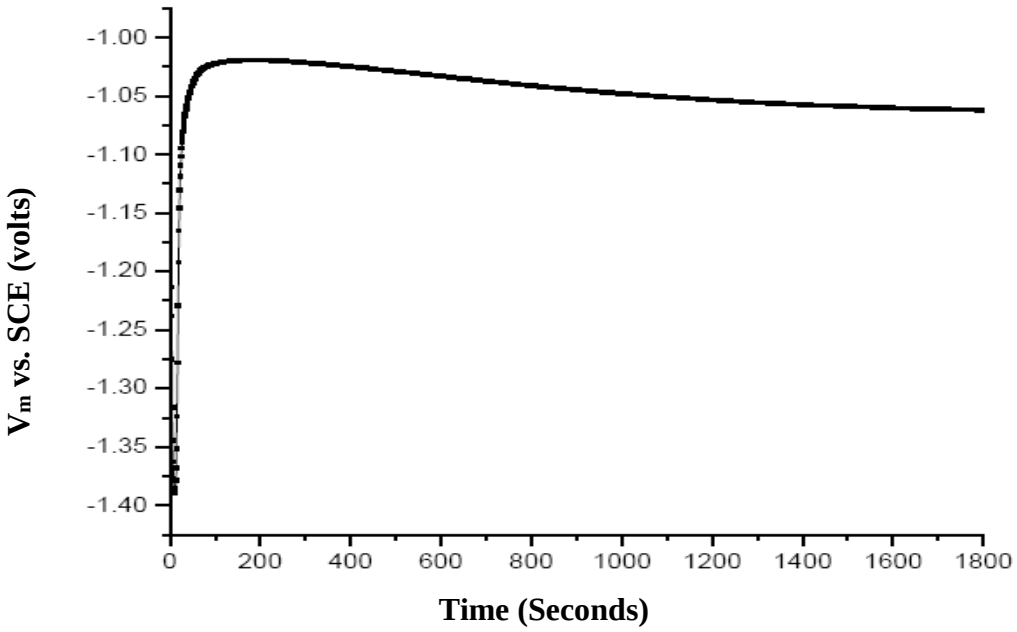

Figure 4.3 Experimental Galvanostatic curve during electrodeposition process

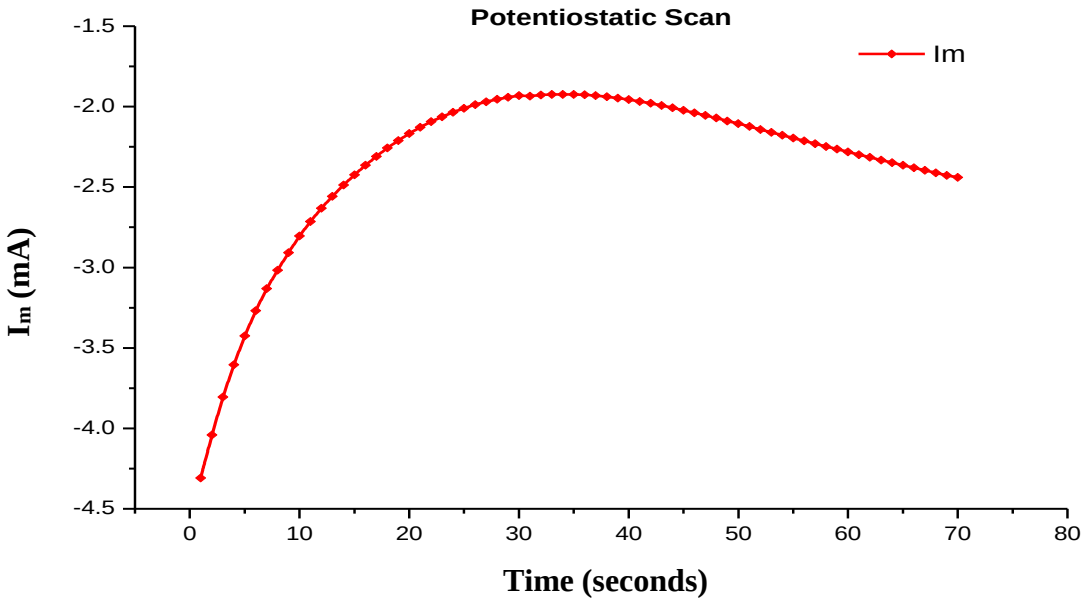

Figure 4.4 Experimental Potentiostatic curve during electrodeposition process

4.3 Post Electrodeposition treatment of substrate

The electrodeposited substrate was washed with DMW jet several times and then it was allowed to dry in air at room temperature. The samples were characterized first without heat treatment and then were annealed up to 250 ºC @ 5 °C/min in air. Annealing was performed in muffle furnace for 03 hours with each sample. Annealing was performed for two purposes, one is to convert any residual metallic nickel and nickel hydroxide present in the substrate into nickel oxide and secondly to improve the adhesion of the deposited film with the substrate.

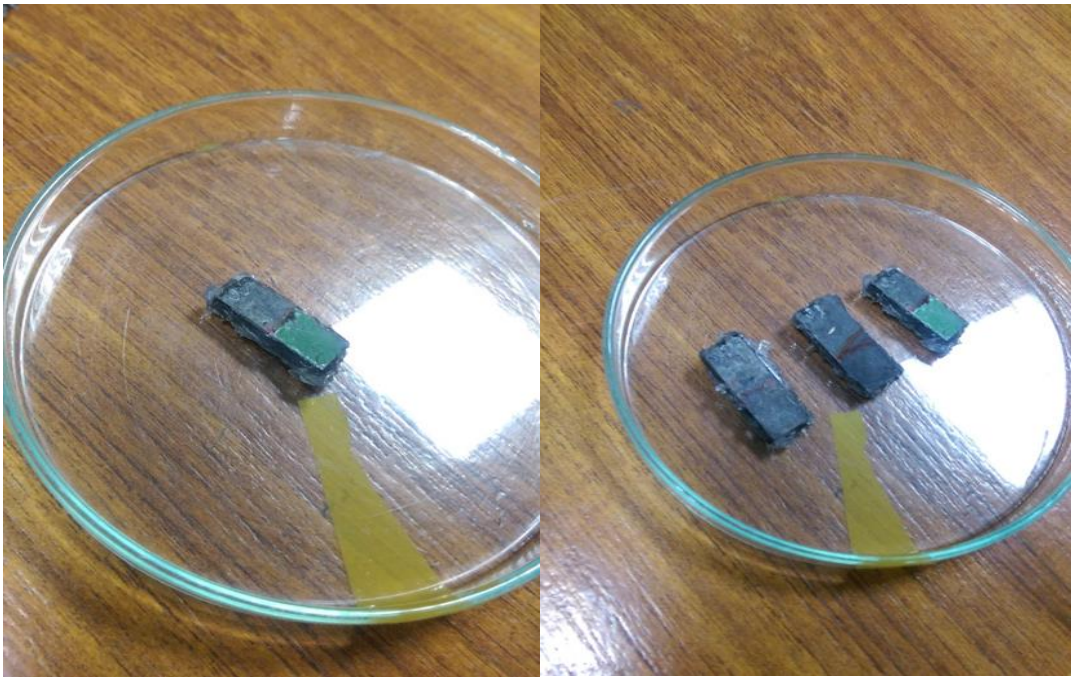

Figure 4.5. Photographs of as deposited NiO films. (having a surface area of 10 X 10 mm each)

Table 4.1. Experimental details of initial experimental set up

Sample ID	**Deposition Time**	**Deposition Mode**	**Applied Potential** (vs. SCE/Ref. Electrode)
01	01 min	Potentiostatic	-0.9V
02	05 min	Potentiostatic	-0.9V
03	08 min	Potentiostatic	-0.9V
04	15 min	Potentiostatic	-0.9V

Table 4.2. Experimental details of final experimental set up

Sample ID	**Deposition Time**	**Deposition Mode**	**Applied Potential** (vs. SCE/Ref. Electrode)
A	10 min	Potentiostatic	-0.9 V
B	20 min	Potentiostatic	-0.9 V
C	15 min	Galvanostatic	-2.1 mA
D	20 min	Galvanostatic	-2.1 mA
E	30 min	Galvanostatic	-2.1 mA

In the first phase, 04 samples were electrodeposited in Potentiostatic mode at an applied potential of -0.9V vs, SCE by using the GAMRY FRAMEWORK Experimental software toolkit. The electrodeposition was carried out for 01,05,08 and 15 minutes for samples 1,2,3 and 4 respectively, as mentioned in Table 4.1.

Based on results obtained from the first 04 samples, experimental plan was revised and five more samples were made. The first two samples were made in the Potentiostatic mode by increasing the deposition time and the remaining 03 samples were made in the Galvanostatic mode which is a fast deposition process. A constant current of -2.1mA was applied to the working electrode for the required deposition time as mentioned in Table 4.2.

.

Chapter 5

Results and Discussion

5.1 Electrochemical characterization of Nickel Oxide Films on carbon plate

The electrochemical properties of Electrodeposited NiO on carbon substrate were investigated primarily by cyclic voltammetry technique. Standard three electrode system was employed for recording CV with following cell arrangement;

- ✓ carbon plate (Conductor) substrate as working electrode (WE)
- ✓ SCE as a reference electrode (RE)
- ✓ Graphite rod as a counter electrode (CE)

The CV curve of bare carbon electrode is shown in Figure 5.1. There is no change in the shape of the curve by increasing the scan rate from 50mV/s to 100mV/sec. Also it shows no anodic and cathodic peaks with a simple closed loop. This behavior implies that bare carbon electrode possesses EDLC, a characteristic of conventional capacitors.

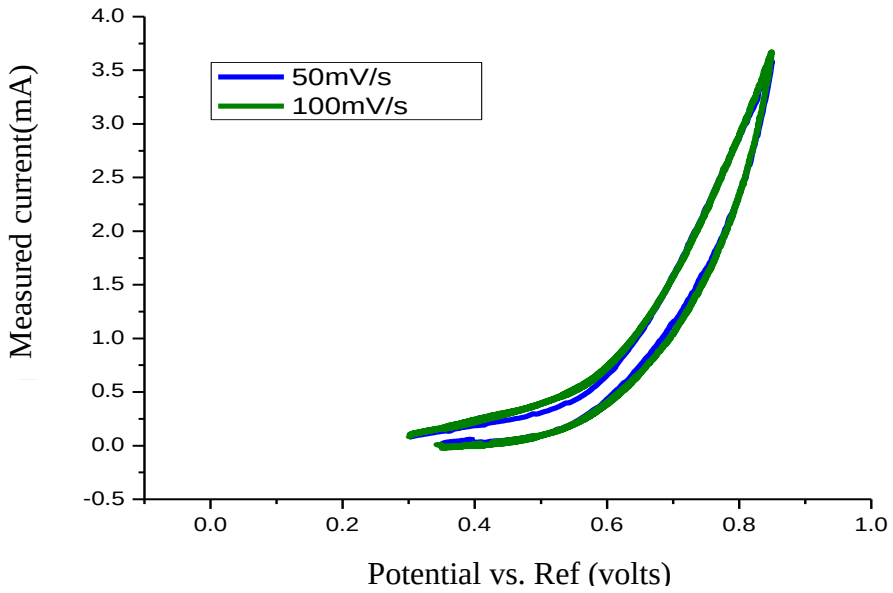

Figure 5.1 Cyclic voltammograms of bare carbon electrode in 1M KOH solution at different scan rates

The capacitance of NiO_x film was determined from following Equation;

$$C = dQ/dV = I/(dV/dt) \quad (5.1)$$

Where "C" is the capacitance of electrode, "Q" is the charge on the electrode; "V" is its potential, "I" is the average current and "dV/dt" is the voltage scanning rate.

Finally, the specific capacitance was calculated by dividing the capacitance of the electrodeposited film electrode by its relevant weight. The weight of the deposited film was found by using a microbalance.

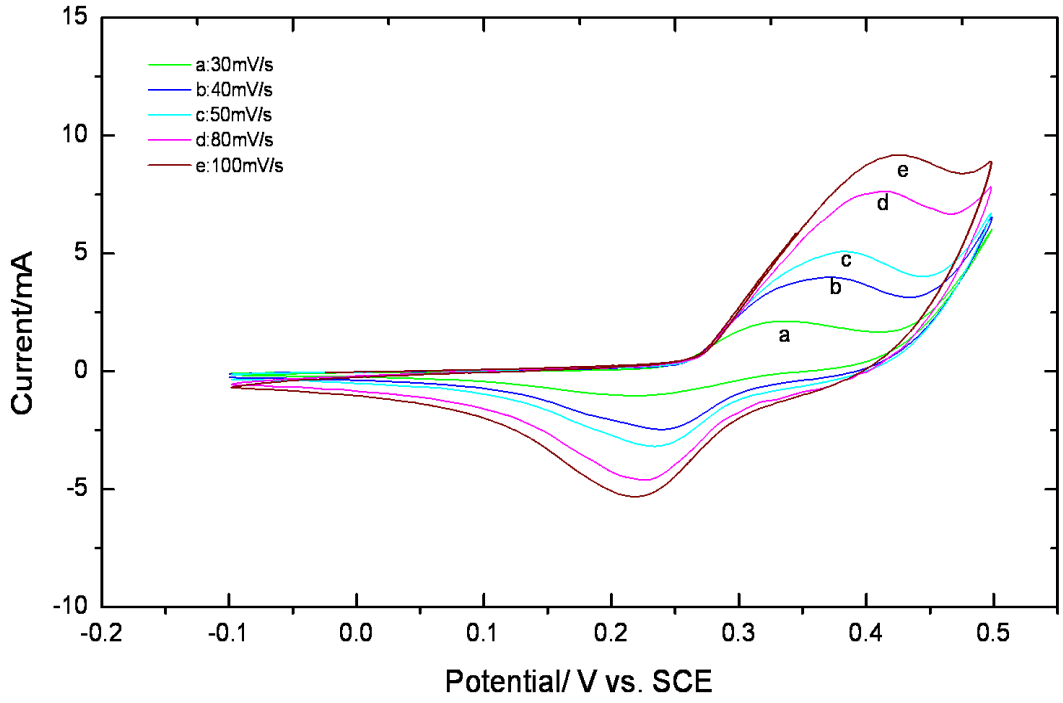

Figure 5.2 Cyclic voltammograms of NiO_x modified carbon electrode in 1M KOH solution at different scan rates, (a) 30 (b) 40 (c) 50 (d) 80 and (e) 100mV/s.

The CV curves of electrodeposited NiO_x film after annealing at 250 ^{0}C are illustrated at various scan rates in Figure 5.2. Cyclic voltammetry was performed in a large potential window of-0.1V to +0.5V vs. SCE in1MKOH aqueous electrolyte. The

shape of the curve is found to be asymmetric with anodic and cathodic peaks illustrating the redox process at electrode electrolyte interface which is characteristic of pseudo capacitance behavior observed in supercapacitors. These two significant peaks appear because of the popular Faradaic reaction of nickel oxide film which proceeds as per following mechanism.

$$NiO + OH^- \Longleftrightarrow NiOOH + e^- \quad (1)$$

This semi-reversible one electron transfer reaction is observable in each curve, verifying that the assessed capacitance is based on redox process. This behavior of oxide film electrode differentiates it from the bare carbon electrode whose CV curve shows no anodic and cathodic peaks with a simple closed loop as shown in Figure 5.1. It is seen from the figure that curves broaden by increasing the scan rate, implying that the current is proportional to the sweep rate which is an indicator of the good capacitive behavior of material. Moreover, the typical shape of the CV curve of electrodeposited film does not alter considerably by increasing the scan rate. It points towards an optimum capacitance performance of electrode material, small ESR (Equivalent series resistance) as well as the accelerated diffusion of ions into the porous thin film.

The variation of maximum anodic current *vs*. scan rate is plotted in Fig 5.3 which shows an almost linear relationship. This behavior is a typical characteristic of the perfect supercapacitor electrode materials. This response of material also implies that $Ni(OH)_2$ present in the as synthesized film is converted to NiO after annealing at 250^0C because in hydroxides anodic peak current(i_p) varies linearly with $V^{1/2}$ independent of the scan rate.

5.2 Structural Characterization (XRD) of Electrodeposited film

After synthesis of thin films, their structural characterization was performed by XRD. The XRD pattern for all the 04 samples electrodeposited during the initial experimental set up in Potentiostatic mode was almost similar and shown in Figure 5.4. All the peaks found were associated with carbon substrate at 2Θ=26.4,44.4,54.5,59.7,77.20 in agreement with JCPDS No. 41-1487 without identification of any peaks related with coating material characteristic pattern like NiO, $Ni(OH)_2$ or Nickel.

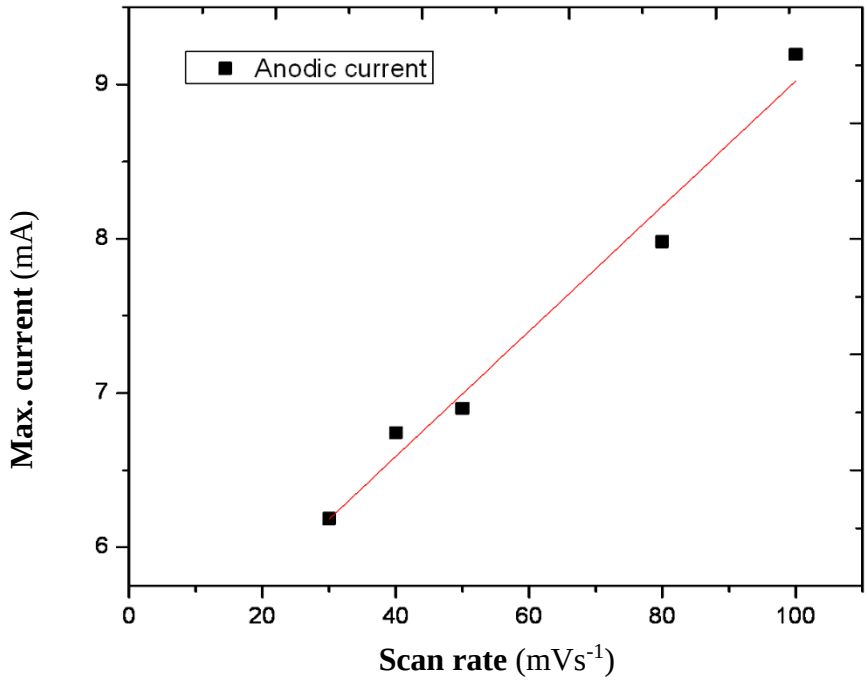

Figure 5.3: The relationship of anodic peak current (i_p) with voltage sweep rate

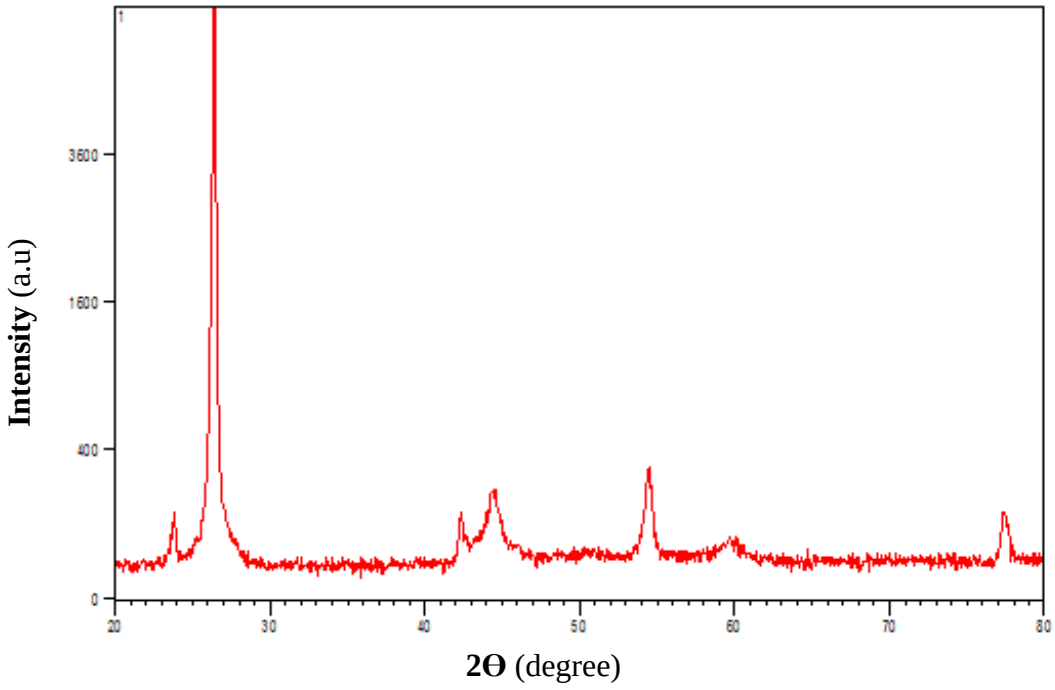

Fig 5.4. XRD pattern of electrodeposited samples in initial experimental set up

The XRD (X-ray Diffractometer, Model STOE θ-θ) results of the NiO film deposited on carbon plate in the final experimental set up are shown in Figure 5.5. The peaks observed at26.4°,44.4°.54.5°,59.7° and 77.2° stand for carbon in the substrate (JCPDS, No.41-1487). NiO peak was observed at 2θ=43.2° corresponding to (200) diffraction plane (JCPDS, No.22-1189) that verifies the cubic NiO_x present in the sample. α-$Ni(OH)_2$ is also observed corresponding to (006) and (110) diffraction planes (JCPDS, No.38-0715) at 2θ = 23.6°and 59.8 ° respectively. The formation of Ni(OH)2 may be attributed to the presence of intercalated water or moisture at the substrate surface. The film which is amorphous in nature has smaller crystallite size than crystalline structured films. Initially the color of deposited films was green which was transformed into black after heating at 250°C. The color change may be attributed to conversion of stoichiometric to non- stoichiometric character of nickel oxide.

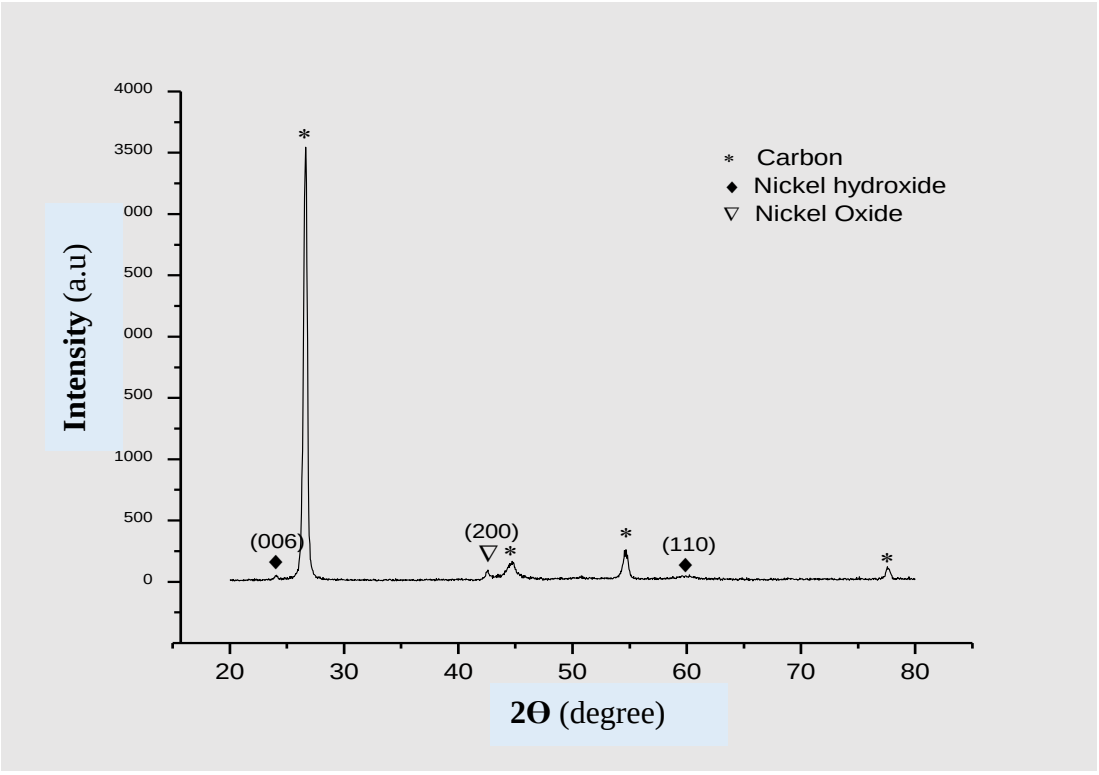

Fig 5.5. XRD pattern of electrodeposited samples in final experimental set up

5.3 Microstructural Characterization and Chemical Composition

The microstructures of coated samples synthesized during initial experimental set up in Potentiostatic mode are shown in Fig 5.6. The sample 1 revealed no coating at all and simply showed the morphology of bare carbon electrode. The sample 2 showed some dispersed nano sized particles but with no uniform coating.

Sample 1 (1 min)

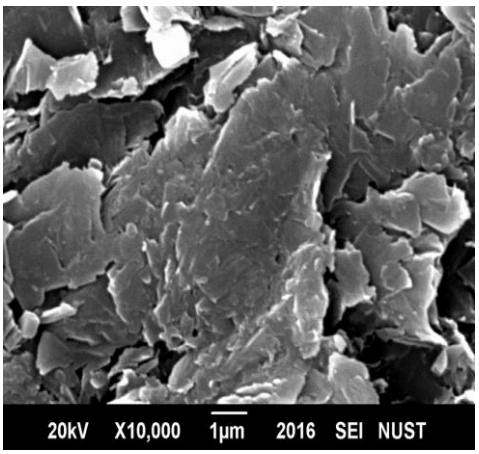

Sample 2 (5 min)

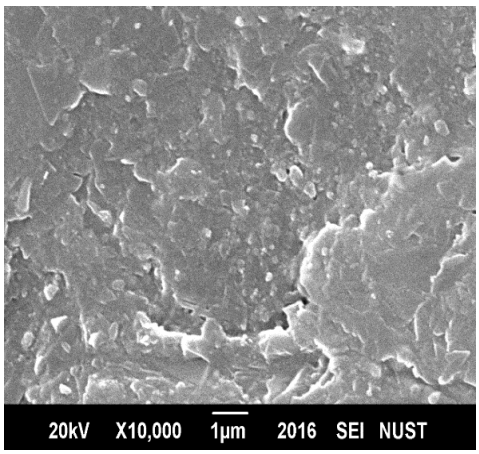

Sample 3 (8 min)

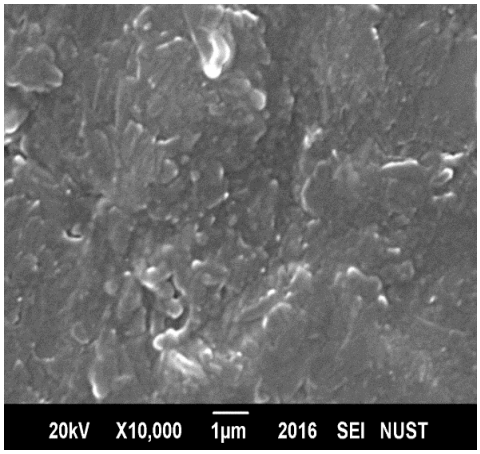

Sample 4 (15min)

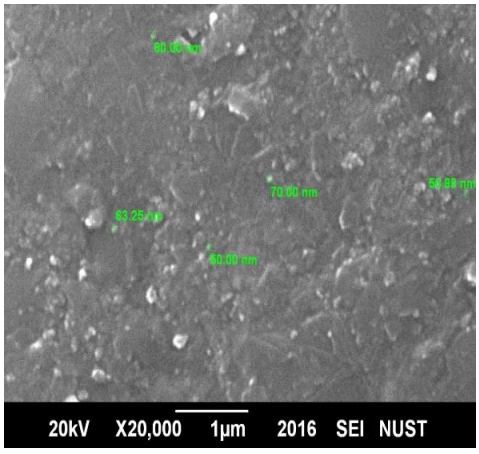

Fig 5.6: SEM images of electrodeposited samples synthesized at different deposition times in Potentiostatic mode during initial experimental set up

The comparison of sample 3 and sample 4 shows that by increasing the deposition time from 8 minutes to 15 minute. more nanoparticles are found to be coated on the substrate ranging in the size of 50~80nm but these ultrafine particles did not uniformly cover the substrate to form a uniform thin film.

SEM figures of as deposited samples in Galvanostatic mode and then annealed at 250 ^{o}C are illustrated in Figure 5.7. The electron microscopy of the as synthesized particulate thin film is illustrated in Figure1.The surface morphology of bare carbon substrate is shown in Fig.5.7(a). As observed from Fig.5.7 (b), the substrate was found to be uniformly coated with dense submicron particles. The high specific surface area of this morphology is complimentary for EC supercapacitors. The crack seen in the image is caused by the shrinkage of the film during air drying after deposition. As deposited films hold a significant amount of moisture, so upon drying residual stresses are developed in the material due to shrinkage which may cause some cracking in the film.

Earlier it is described that the films having a thickness of >0.2 µm usually show some cracks in the structure. An example of this phenomena occurs in ZrO_2 thin films as well as for Molybdenum Oxide to be deposited by Galvanostatic conditions The SEM image in Fig5.7(c) depicts a loosely packed porous structure of NiO particles which ensures the high surface area required for efficient contact between the film and the electrolyte during redox reaction. This type of structure eases the movement of electrolyte ions not only at the external region of the electrode surface but also into the internal areas thus increasing the active area of the film participating in the redox reaction. This phenomenon enhances the redox reaction rate resulting in increase of capacitance of the electrode. The film shows dense and granular morphology of interconnected particles having size in the range of approximately 550 ~ 850 nm as could be seen in Fig5.7 (d). The thickness of the particulate film is portrayed in Fig 5.7(e) which demonstrates an almost uniform average thickness of 2.9 µm having loosely crowded submicron spherical particles. At higher temperatures, grain size increases and the particles agglomeration takes place as shown in micrograph of NiO annealed films in Fig 5.7(f). The image shows dense aggregation of particles.

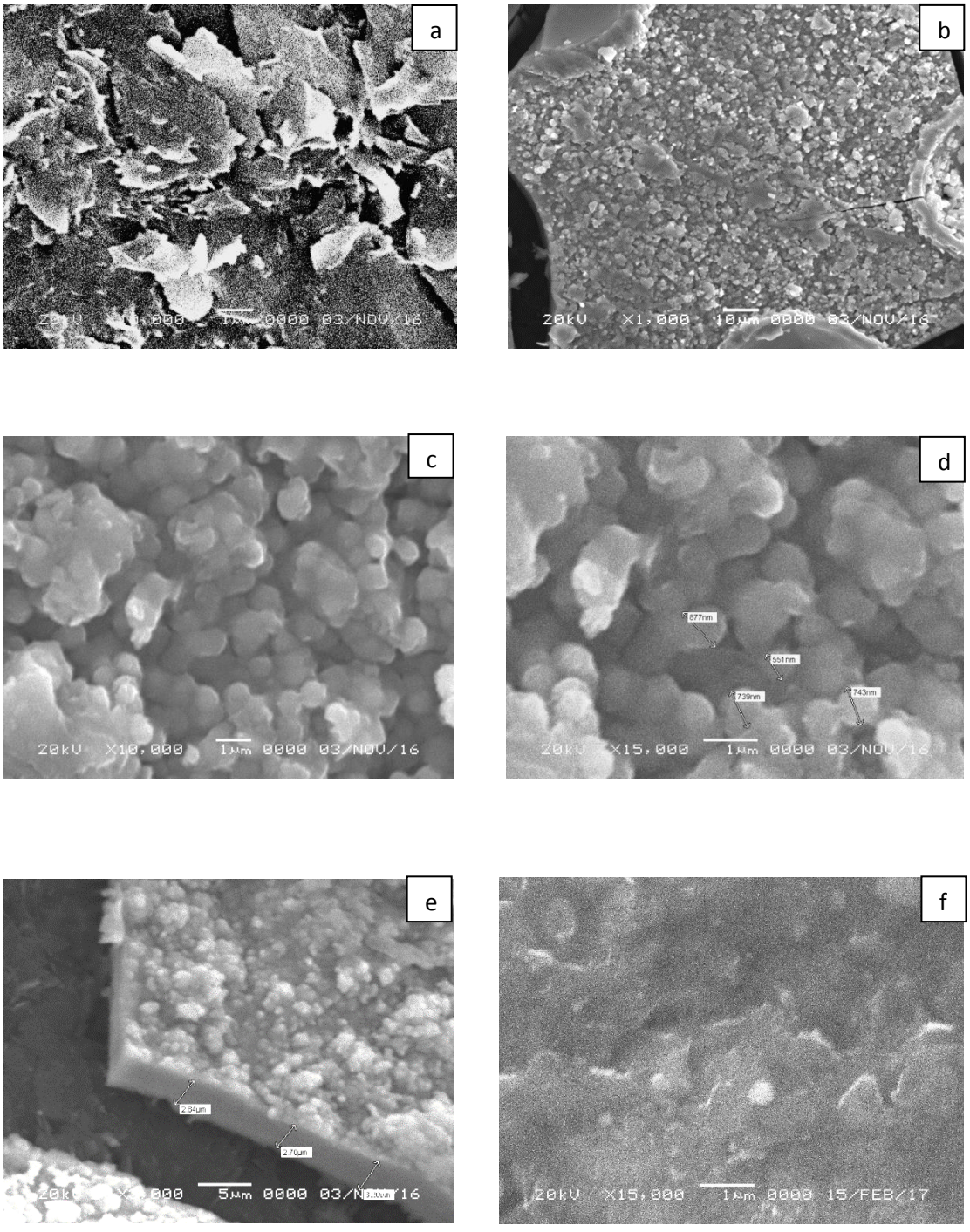

Fig 5.7: SEM images of **(a)** carbon substrate **(b& c)** as synthesized film **(d)** measurement of film particle size **(e)** measurement of film thickness **(f)** annealed film

The EDX spectrum of thin film verify the existence of Nickel and Oxygen in bulk concentrations. This is shown in Fig 5.8.

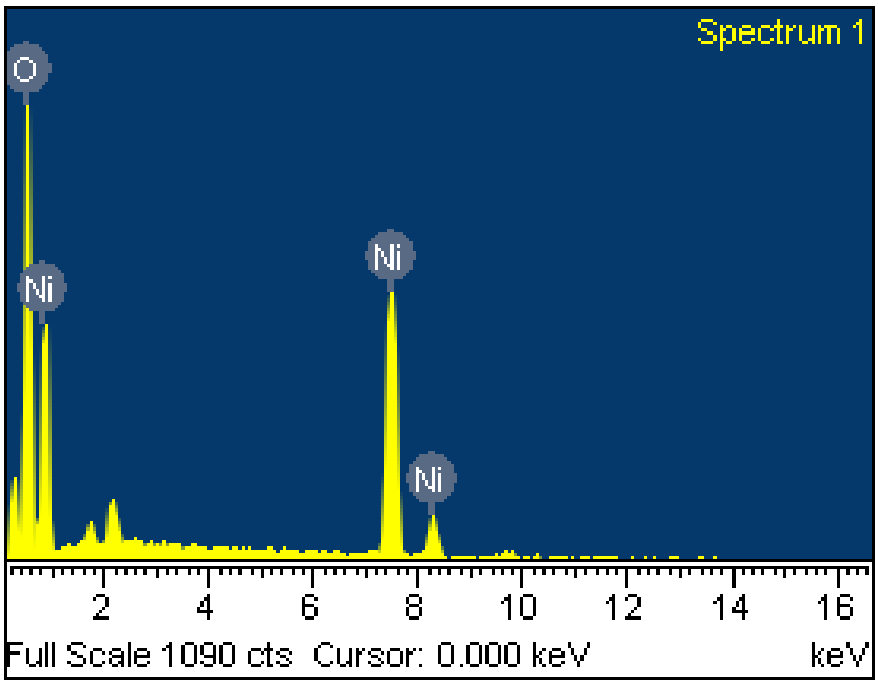

Fig. 5.8 EDX spectrum of NiO_x film

The atomic and weight percentages of Ni and O in the electrodeposited film are quantified in Table 5.1. The surface composition of the film was found to be $Ni_{0.32}O_{0.68}$ by considering the atomic ratios of Ni and O in the spectrum.

Table 5.1 Extent (wt. %) of Nickel and Oxygen in nickel oxide films

Element	Weight %	Atomic %
O	37.15	68.44
Ni	62.85	31.56
Totals	100.00	100.00

Conclusions

The NiO thin film containing submicron granular shaped interconnected particles was deposited electrochemically on conducting carbon plate in a chemical bath of Nickel Nitrate hexahydrate. The scanning electron microscopy exposed that the film consists of submicron particles with a uniform coverage on carbon electrode. Porosity has also been found between the particles which confirms the maximum electrode electrolyte interfacial contact throughout the redox process owing to fast charging of supercapacitors in application. The XRD peaks confirmed the existence of NiO in the film. The EDX spectrum exhibited the quantitative analysis of surface composition for NiO film and found to be $Ni_{0.32}O_{0.68}$ The CV interpretation of electrodeposited annealed film was done to calculate a specific capacitance of 254F/g at a scan rate of 30mV/s. Therefore, electrodeposition is a simple and reliable technique through which the specific capacitance of carbon plate can be enhanced from 4 F/g to 254 F/g by deposition of nickel oxide film for supercapacitor applications. The relatively low cost of carbon material brands NiO modified carbon electrode as an economical optimal for use as a positive electrode in supercapacitor device.

Future Work

- Indigenous development of Supercapacitor device with NiO modified carbon as positive electrode and Co_3O_4 as a negative electrode.
- Performance evaluation of device through electrochemical characterization.
- Calculation of Energy and Power density of device.

References:

[1] A.B. Soto, E.M. Acre, M. Palomar-Pardave and I. Gonzalez, *Electrochim. Acta*, 41(**1996**)2647.

[2] C.Q, Sui, S.P. Jiang and A.C.C. Tseung, *J. Electrochem. Soc*.,137(**1990**)3418.

[3] C.H. Liang and C.S. Hwang, *J. Alloys Compd*., 102(**2010**)500.

[4] B. Babakhani and D.G. Ivey, *Journal of Power sources*.,196(**2011**),10762.

[5] S. Sarangapani, B.V. Tilak and C.-P. Chen, *J. Electrochem. Soc*.,143(**1996**) 3791.

[6] Hae-Min Lee, Kangtack Lee and Chang-Koo Kim, *Materials,* 7(**2014**),265.

[7] S. Trassati and P. Kurzweil, *Platinum Met,* Rev, 38(**1991**) 46.

[8] B.E. Conway, *J. Electrochem*. Soc., 138 (**1991**) 1539.

[9] Zheng, J.P., Cygan, P.J. and Jow T.R., *J. Electrochem. Soc.*, 142 (**1995**) 2699.

[10] D.B. Wang, C.V. Song, Z.S. Hu and X. Fu, *J.Phys. Chem. B*, 109 (**2005**) 1125.

[11] J.W. Lang, L.B. Kong, W.J. Wu, Y.C. Luo and L. Kang, *Chem. Commun*., 35 (**2008**) 4213.

[12] M.J. Deng, F.L. Huang, I.W. Sun, W.T. Tsai and J.K. Chang, *Nanotechnology*, 20 (**2009**) 175602.

[13] L.Cao, F. Xu, Y.Y. Liang and H.L. Li, *Adv. Mater*., 16 (**2004**) 1853.

[14] Hong-Ying Wu and Huan-Wen Wang, *Int. J. Electrochem. Sci.*, 7 (**2012**) 4405.

[15] S.M. Lindasy, Introduction to Nanoscience, Oxford University Press. (**2010**) 285.

[16] Reiss. H. and A. Heller, *J.Phys. Chem.*, 89 (**1985**) 4207.

[17] Martin winter and Ralph Brodd, What are Batteries, Fuel cells and Supercapacitors, *Chem.Rev.*,104 (**2004**) 4245.

[18] B.E. Conway, Electrochemical supercapacitors, scientific fundamentals and Technological Application, Plenum Press, New York (**1999**).

[19] Simon P and Gagosti Y, *Nat. Mat*., 7 (**2008**) 845.

[20] Marcus R.A., *J. Phys. Chem.*, 43 (**1965**) 679.

[21] Conway BE, *J. Electrochem. Soc.*, 138 (**1991**) 1539.

[22] Sarangapani S. Tilak and BV. Chen C.P., *J. Electrochem. Soc*.,143 (**1996**) 3791.

[23] Hae-Min Lee, Kangtack Lee and Chang-Koo Kim, *Materials*, 7 (**2014**) 265.

[24] Farrukh Iqbal Dar, Kevin Ramakrishna Moonoo Swamy and Mohammed Es-Souni, Morphology and property control of NiO nanostructures for supercapacitor applications, *Nanoscale Research Letters*, 8 (**2013**) 363.

[25] Rudge A., Davey J., Raistrick I., Gottesfeld S. and Ferrais J.P., Conducting polymers as active materials in electrochemical capacitors, *J. Power Sour*., 47 (**1994**) 89.

[26] Cahing C.K., C.R. Fincher, Y.W. Park, H. Shirakawa, E.J. Louis, S.C. Gau and McDiarmid, Electrical conductivity in doped polyacetylene, *Phys. Rev. Lett*.,39 (**1977**) 1098.

[27] Ke YF, Tsai DS and Huang YS, Electrochemical Capacitors of RuO_2 nanophase grown on $LiNbO_3$(100) and sapphire (0001) substrates, *J. Materials Chem.*,15 (**2005**) 2122.

[28] Zheng JP and Jow TR, A new charge storage mechanism for electrochemical capacitors, *J. Electrochem. Soc.*, 142 (**1995**) L6.

[29] Lang JW, Kong LB, Wu WJ, Luo YC and Kang L, *Chem. Commun.*, 35 (**2008**) 4213.

[30] Patil UM, Gurav KV, Fulari VJ, Lokhande CD and Joo OS, Characterization of honeycomb like, β-$Ni(OH)_2$, thin films synthesized by chemical bath deposition method(CBD)and their supercapacitor application, *J. Power Sources*, 188 (**2009**)338.

[31] Fisher AE, Pettigrew KA, Rolison DR, Stround RM, Long JW, Incorporation of homogeneous, nanoscale MnO2 within ultraporous carbon structures self-limiting electroless deposition, implications for electrochemical capacitors, Nano Lett., 7(**2007**)281.

[32] Zheng MB, Cao J, Liao ST, Liu JS, Chen HQ, Zhao Y, Dai WJ, Ji GB, Cao JM and Tao J, Preparation of mesoporous Co_3O_4 nanoparticles via Solid-Liquid route and effects of calcination temperature and textural parameters on their electrochemical capacitive behaviors, *J. Phy. Chem.* C, 113 (**2009**) 3887.

[33] Lee HY and Goodenough JB, Ideal supercapacitor behavior of amorphous $V_2O_5.nH_2O$ in potassium chloride (KCI) aqueous solution, *J. Solid state Chem.*, 148 (**1999**) 81.

[34] D.A. Brownson, D. K. Kampouris and C.E. Banks, *Journal of Power Sources*,196

(**2011**) 4873.

[35] Safina Iram Javed, Zakir Hussain, Covalently Functionalized Graphene Oxide-Characterization and its Electrochemical Performance, *International Journal of Electrochemical Science*, 10 (**2015**) 9475.

[36] Greenwood, Norman N, Earnshaw and Alan, Chemistry of the Elements (2^{nd} Ed.), Pergamon Press, Oxford (**1997**).

[37] Jin-Kyu Kang and Shi-Woo Rhee, Thin solid films, 391(**2001**) 57.

[38] R. Polambari, *J. Electroanal. Chem.*, 23 (**2003**) 546.

[39] C.M. Lambert, G. Nazri and P.C. Yu, *Sol. Energy Mater*.,16 (**1987**) 1.

[40] N. Shaigan, D.G. Ivey and W. Chen, *J.Electrochem.Soc*.,155 (**2008**) D278.

[41] E. Avendano, L. Berggren, G.A. Niklasson and C.G. Granqvist, *Thin solid films*,496 (**2006**) 30.

[42] A.C. Sonavane, A.I. Inamdar, P.S. Shinde, H.P. and Deshmukh R.S. Patil, *J. Alloys compds*.,489 (**2010**) 667.

[43] H. Kamel, E.K. Elmaghraby, S.A. Ali and K. Abdel-Hady, *Thin solid films*,483 (**2005**) 330.

[44] Liang K, Tang X and Hu W, High-performance three-dimensional nanoporous NiO film as a supercapacitor electrode, *J. Mat. Chem*., 22 (**2012**) 11062.

[45] Farrukh Iqbal Dar, Kevin Radakishna, Moonoo Swamy and Mohammed Es-Souni: Morphology and property control of NiO nanostructures for supercapacitor applications. *Nanoscale Research Letters*, 8 (**2013**) 363.

[46] M.S. Wu and H.H. Hsieh, *Electrochim. Acta*,53 (**2008**) 3427.

[47] Venkat Srinivasan and John W. Weidner, *J. Power sources*,108 (**2002**) 15.

[48] Xiong S, Yuan C, Zhang X and QianY, *Cryst. Eng. Comm.*,13 (**2011**) 626.

[49] Miller EL and Rocheleau RE, Electrochemical behavior of reactively sputtered iron-doped nickel oxide, *J. Electrochem. Soc*., 144 (**1997**) 3072.

[50] J.B. Gerken, J.G. McAlpin, J.Y.C. Chen, M.L. Rigsby, W.H. Casey, R.D. Britt and S.S. Stahl, *J. Am. Soc*., 133 (**2011**) 14431.

[51] AIex Izgorodin, E. Izgorodina and Douglas R. Macfarlane, *Energy Environ. Sci.*, 5 (**2012**) 9496.

[52] S. Trasatti, *Electrochimica Acta*, 45 (**2000**) 2377.

[53] R Cerc Korosec and P. Bukovec, *Acta Chim. Slov*.,53 (**2006**) 136.

[54] K. D. Lee, W.C. Jung and J. Kor., *Phys.Soc*.,45 (**2004**) 447.

[55] Siti Zairyan Fakurol Rodzi and Yusairie Mohd., The influence of Deposition temperature on the Electrodeposition of NiO films on ITO glass substrate, IEEE Symposium, DOI**:** 10.1109/SHUSER.2012.6268886 (**2012**).

[56] K.K. Purushotaman and G . Muralidharan, *J. Sol Gel Sci.Technol*.,46 (**2008**) 190.

[57] D. M. Kolb and M.A. Schneeweiss, *Electrochem.Soc. Interface*, 8 (**1999**) 26.

[58] T. Osaka and T. Homma., *Electrochem. Soc. Interface*, 4 (**1995**) 42.

[59] M. J. Deng, F. L. Huang, I. W. Sun, W. T. Tsai, and J. K. Chang, *Nanotechnology*, 20 (**2009**) 175602.

[60] Gang Wu, Ning Li, De-Rui Zhou, Kurachi Mitsuo and Bo-Qing Xu, *J. Solid Stat.Chem*.,177 (**2004**) 3682.

[61] Jayashree R.S. and Kamath P.V., Nickel Hydroxide electrodeposition from nickel nitrate solutions: Mechanistic studies, *J. Power Sour*., 93 (**2001**) 273.

[62] Kissinger Peter and William Heinemann, Laboratory Techniques in Electroanalytical chemistry (2nd Ed.), by Marcel Dekker, Inc., ISBN 0-8247-9445-1, New York (**1996**).

[63] Zoski and Cynthia G., Handbook of electrochemistry, Elsevier Science, ISBN 978-0-444-51958-0 (**2006**).

[64] Brand Allen J. and Larry R. Faulkner, Electrochemical method: Fundamentals and Applications, John Wiley, New York (**1980**).

[65] Nicholson, R.S. and Irving Shain, Theory of Stationary Electrode Polarography: Single Scan and Cyclic Methods Applied to Reversible, Irreversible and Kinetic Systems, *Analytical Chemistry*, 36 (**1964**) 706.

[66] Hae-Min Lee, Kangtack Lee and Chang-K Joo Kim, Electrodeposition of Manganese-Nickel Oxide films on a Graphite sheet for Electrochemical Capacitor Applications, *Materials*, 7 (**2014**) 265.

[67] Elton N. Kaufmann, Characterization of materials (2nd Ed.), John Wiley & Sons, Inc., Vol.1 (**2003**).

[68] Peacharsky V. and P. Zavalij, Fundamentals of powder diffraction and structural characterization of materials, Springer Science, 0-387-2456-7, New York (**2005**).